ENGINEERING RESEARCH INSTITUTE
UNIVERSITY OF MICHIGAN
ANN ARBOR

THE DIFFRACTION OF SHOCK WAVES THROUGH OBSTACLES WITH VARIOUS OPENINGS IN THEIR FRONT AND BACK SURFACES

REPORT 50-3

BY

RUSSELL E. DUFF

ROBERT N. HOLLYER, JR.

SUBMITTED BY

OTTO LAPORTE

Project M720-4

U. S. NAVY DEPARTMENT, OFFICE OF NAVAL RESEARCH
CONTRACT NO. N6 ONR-232, TASK ORDER IV

November 7, 1950

THIS REPORT PUBLISHED

FOR

Armed Forces

Special Weapons Project

for

dissemination to

authorized agencies

THE DIFFRACTION OF SHOCK WAVES THROUGH OBSTACLES WITH VARIOUS OPENINGS IN THEIR FRONT AND BACK SURFACES

I. INTRODUCTION

This report presents the results of a photographic investigation of shock-wave diffraction through models with various openings in their front and back surfaces. Also included is a discussion of a method for determining the strength of shock waves by measurements of limiting Mach configurations.

II. DIFFRACTION OF SHOCK WAVES THROUGH MODELS WITH VARIOUS OPENINGS IN THEIR FRONT AND BACK SURFACES

Three symmetric models were used in this investigation. The outside dimensions of each were 1-1/2" x 4-1/2". The size of the openings in the front and back surfaces was varied: the opening in Model A was 53-1/3 percent of the inside dimension; the opening in Model B was 20 percent of the inside dimension; and the opening in Model C was 5 percent of the inside dimension. Each model was studied at three shock strengths: $1/\xi$ was 1.1, 1.44, and 1.8. Both the shock velocity and the flow velocity behind the shock are given in the following table for each shock strength:

$1/\xi$	U(mm/μsec)	u(mm/μsec)
1.1	.360	.024
1.44	.406	.093
1.8	.449	.152

The figure numbers of the photographs for a particular shock strength and model are given in the following table:

	1.1	1.44	1.8
A	1-5	6-10	11-15
B	16-20	21-25	26-30
C	31-36	37-42	43-48

Figures 36 and 42 show an extremely weak primary shock which has been reflected from both the back and front surfaces.

Caution must be exercised in applying these strictly two-dimensional results to three-dimensional problems. In particular, the shock strength inside an obstacle will be determined by the effective aperture in the front of the obstacle, as shown in Figure α. To a first approximation, the thickness of the separated boundary layer is probably dependent on shock strength and time but not on the geometry of the opening. If this be true, then the effect of the boundary layer will be much more important in the case of a narrow slit than in the case of a square opening in the front of an obstacle.

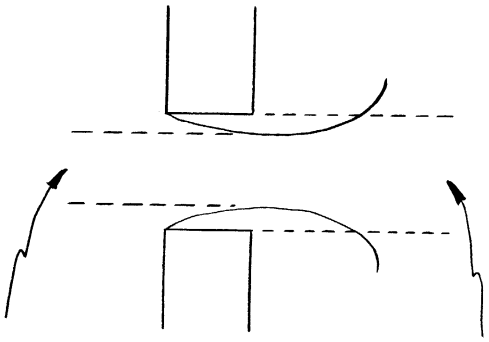

Figure α

III. DETERMINATION OF SHOCK STRENGTH BY MEASUREMENT OF MACH CONFIGURATIONS FOR INFINITESIMAL DEFLECTION

In the analysis of shock-diffraction photographs, one is often confronted with the problem of determining the strength of a shock wave which essentially has undergone reflection through an infinitesimal angle. For instance, this problem arises in several places in this report. Whenever there is a practically plane shock wave followed by a weak reflected shock, as in Figure 8, Mach reflection through an infinitesimal angle may be assumed to have occurred. Lincoln G. Smith[1] calls this the extreme sonic case. It has been called one of the trivial solutions of the general Mach reflection equations by W. Bleakney and A. H. Taub.[2]

A simple analysis is sufficient for the description of this limiting configuration (see Figure β). Assume that an infinitesimal inclination starts at the point b. As the shock, S, passes b, a sound wave is sent out into the flow behind S. This sound wave travels with the speed of sound behind the main shock wave and is swept downstream with the flow velocity u behind the shock wave.

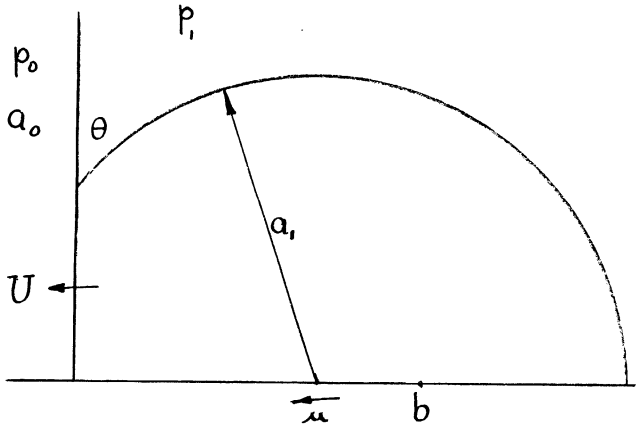

Figure β

---

[1] Lincoln G. Smith, Photographic Investigation of the Reflection of Plane Shocks in Air, NDRC Report No. A-350.

[2] W. Bleakney and A. H. Taub, "Interaction of Shock Waves, Rev. of Mod. Phys. 21 (1949) 584.

The angle θ is given by

$$\cos\theta = \frac{U-u}{a_1}$$

$$\theta = \cos^{-1}\frac{U-u}{a_1}$$

All the velocities appearing in this expression can be expressed as functions of shock strength and gas constants.[3]

$$U = a_o\sqrt{\frac{\mu+\xi}{(\mu+1)\xi}}$$

$$u = a_o\frac{(\mu-1)(1-\xi)}{\sqrt{(\mu+1)\xi(\mu+\xi)}}$$

$$a_1 = a_o\sqrt{\frac{1+\mu\xi}{\xi(\mu+\xi)}}$$

where a_o is sound speed ahead of the shock wave; $\mu = (\gamma+1)/(\gamma-1)$; and $\xi = p_o/p_1$, the shock strength. Thus

$$\theta = \cos^{-1}\left\{\frac{\sqrt{\frac{\mu+\xi}{(\mu+1)\xi}} - \frac{(\mu-1)(1-\xi)}{\sqrt{(\mu+1)\xi(\mu+\xi)}}}{\sqrt{\frac{1+\mu\xi}{\xi(\mu+\xi)}}}\right\}$$

---

[3] F. W. Geiger and C. W. Mautz, The Shock Tube as an Instrument for the Investigation of Transonic and Supersonic Flow Patterns, Report on Contract N6-ONR-232, T.O.IV, 1949.

or

$$\theta = \cos^{-1} \sqrt{\frac{\mu(1-\xi)}{\mu+1}}$$

This function is plotted in Figure γ.

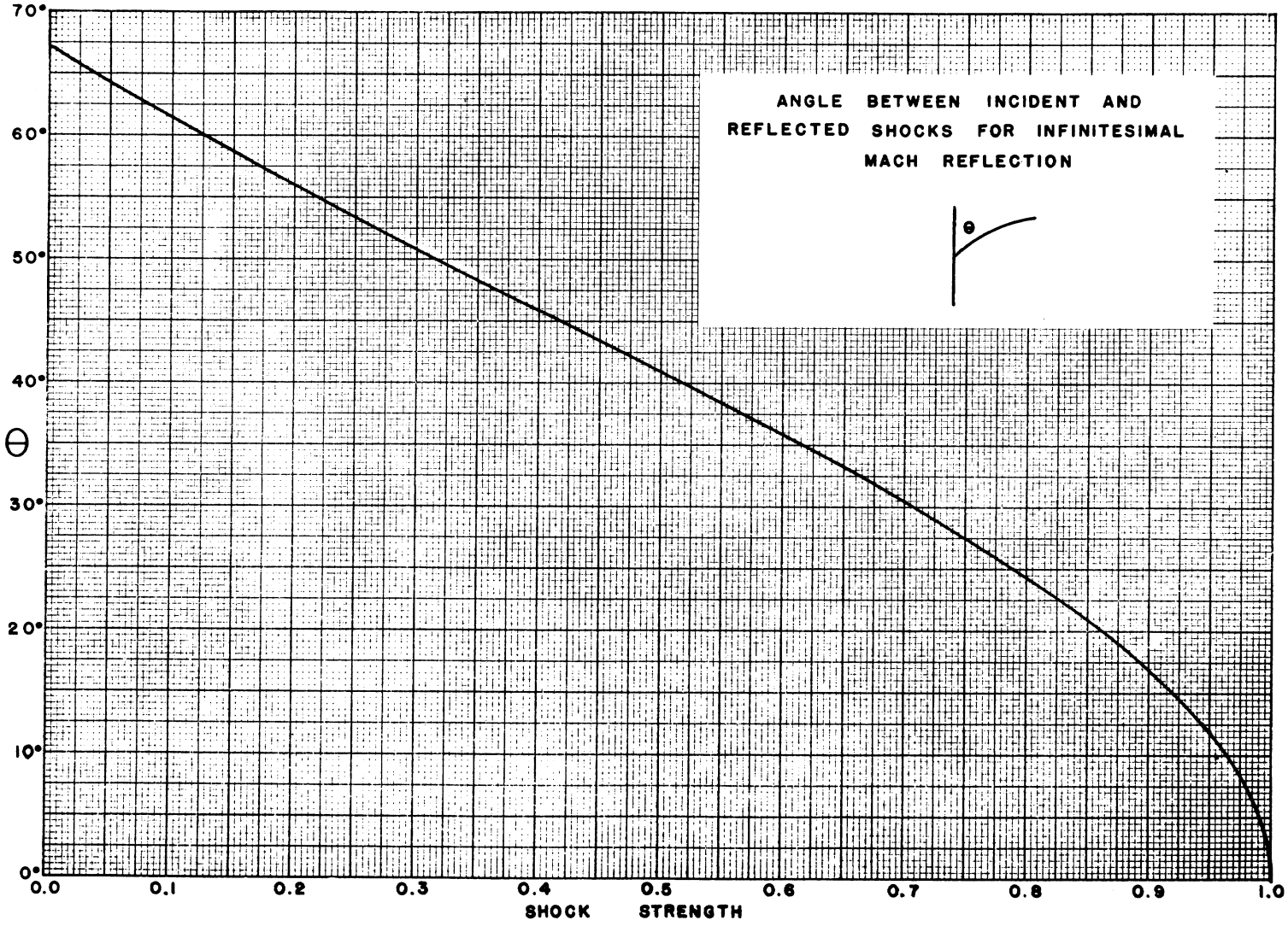
ANGLE BETWEEN INCIDENT AND
REFLECTED SHOCKS FOR INFINITESIMAL
MACH REFLECTION
θ
70°
60°
50°
40°
30°
20°
10°
0°
θ
0.0
0.1
0.2
0.3
0.4
0.5
0.6
0.7
0.8
0.9
1.0
SHOCK STRENGTH

FIGURE 1

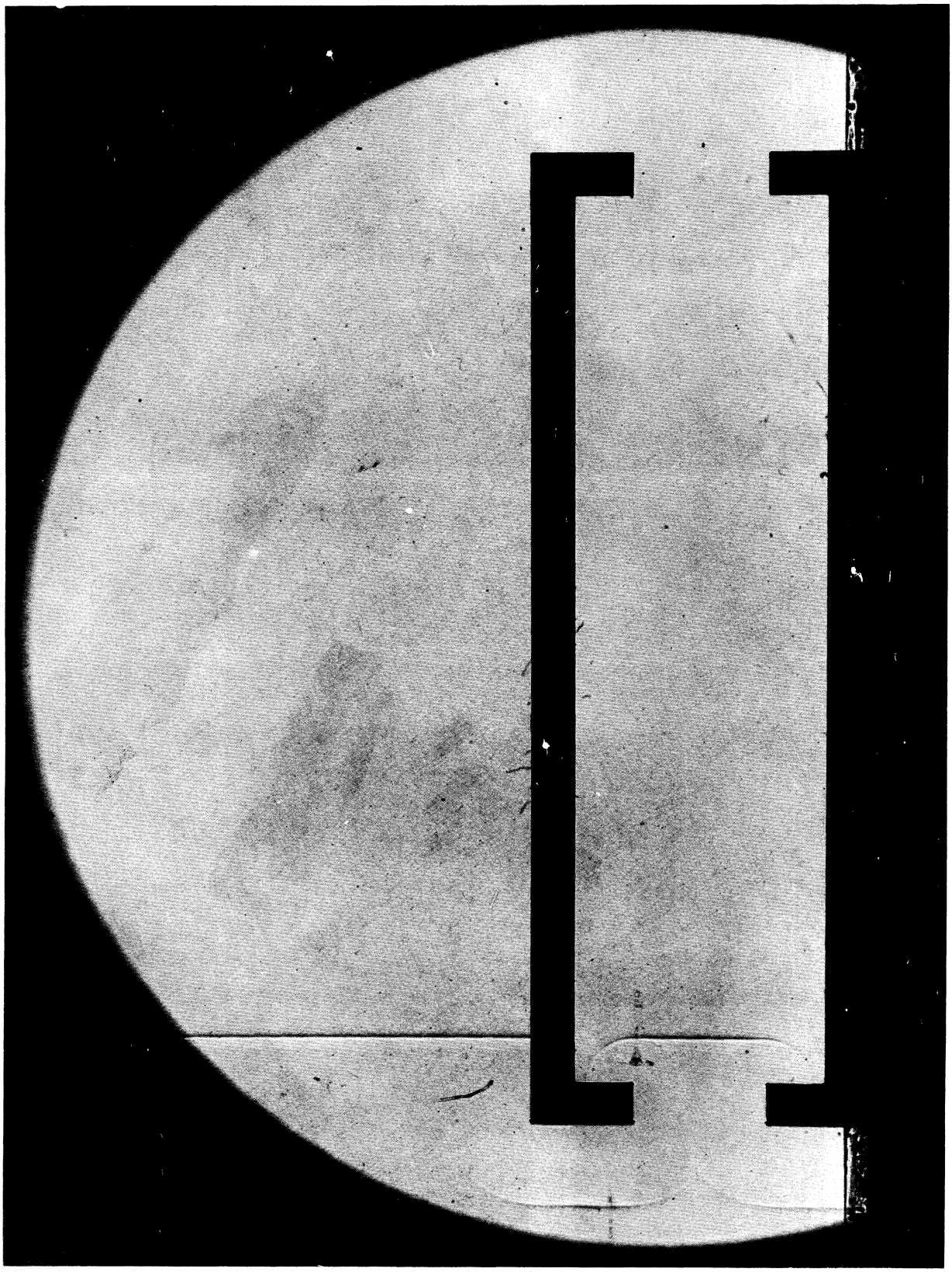

$t = 28$

Figure 1

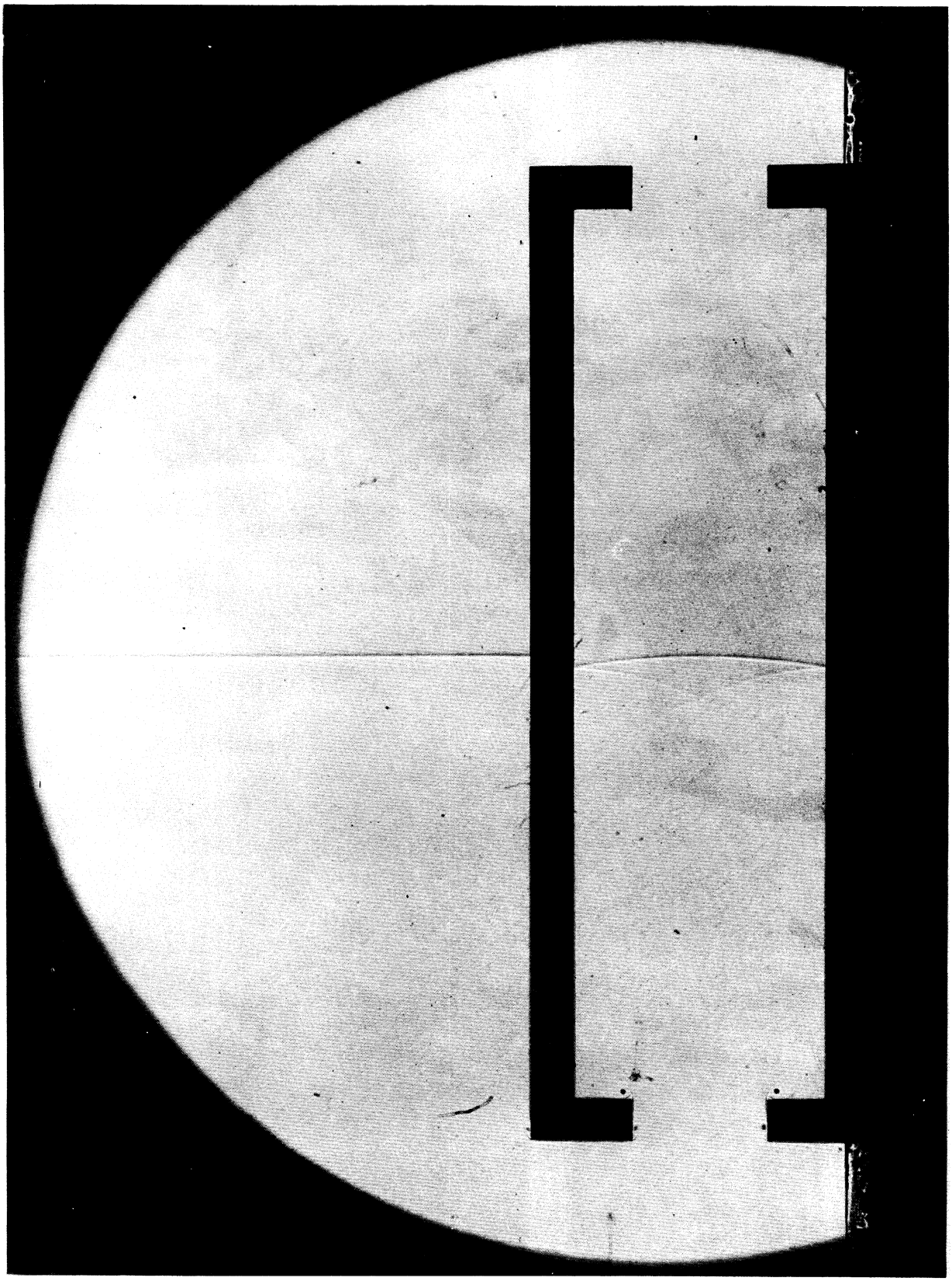

t = 159

Figure 2

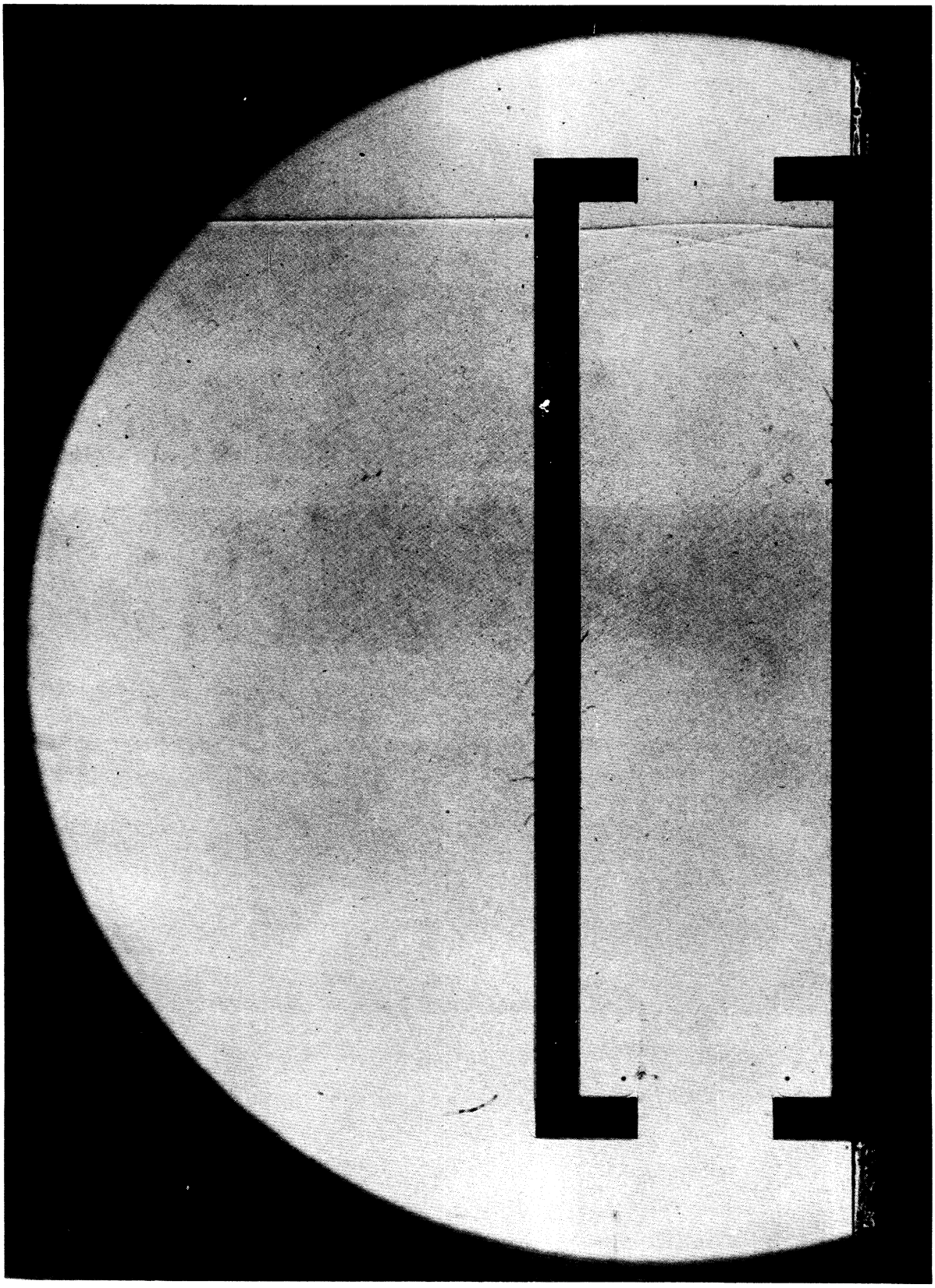

t = 299

Figure 3

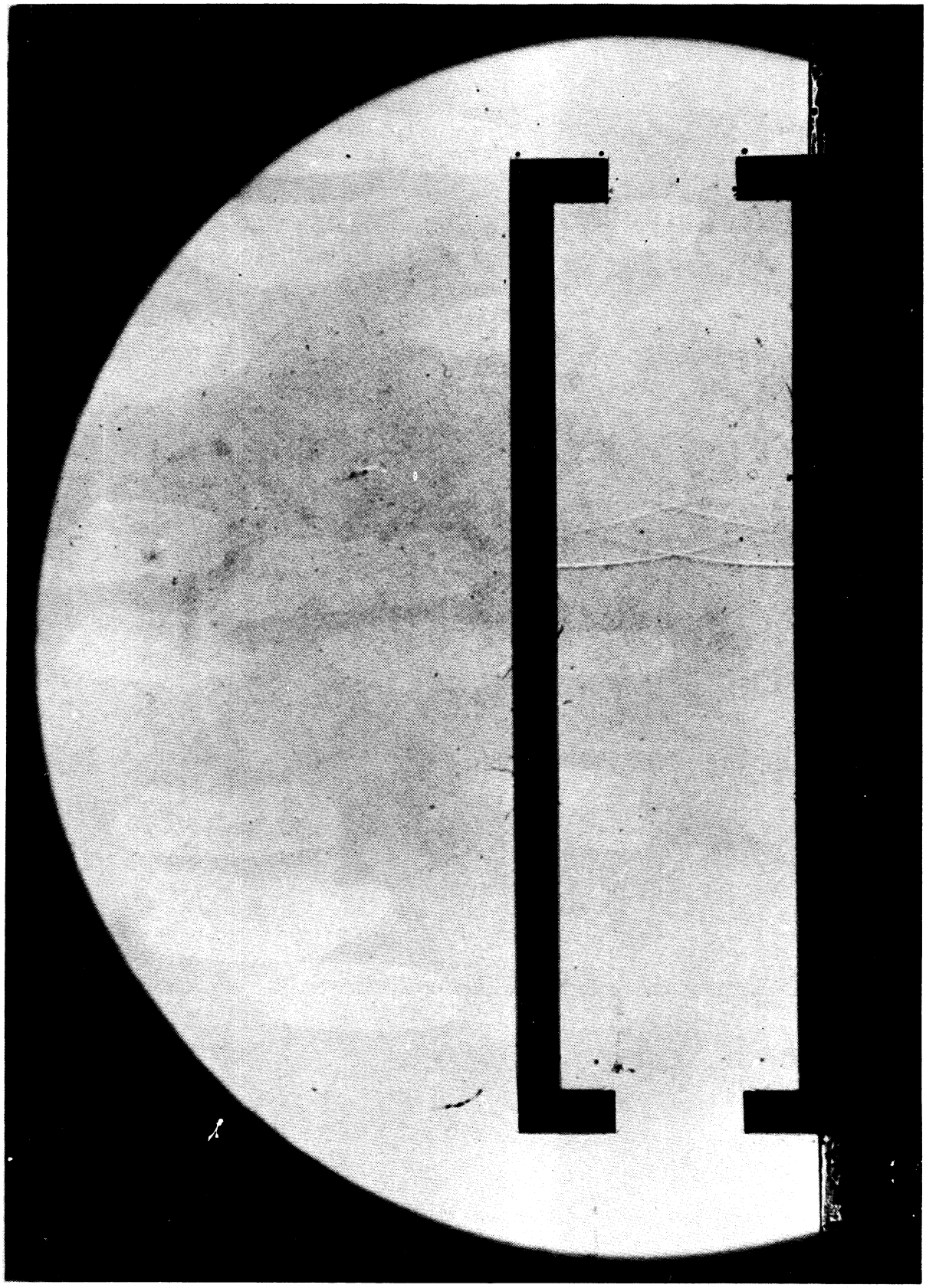

t = 435

Figure 4

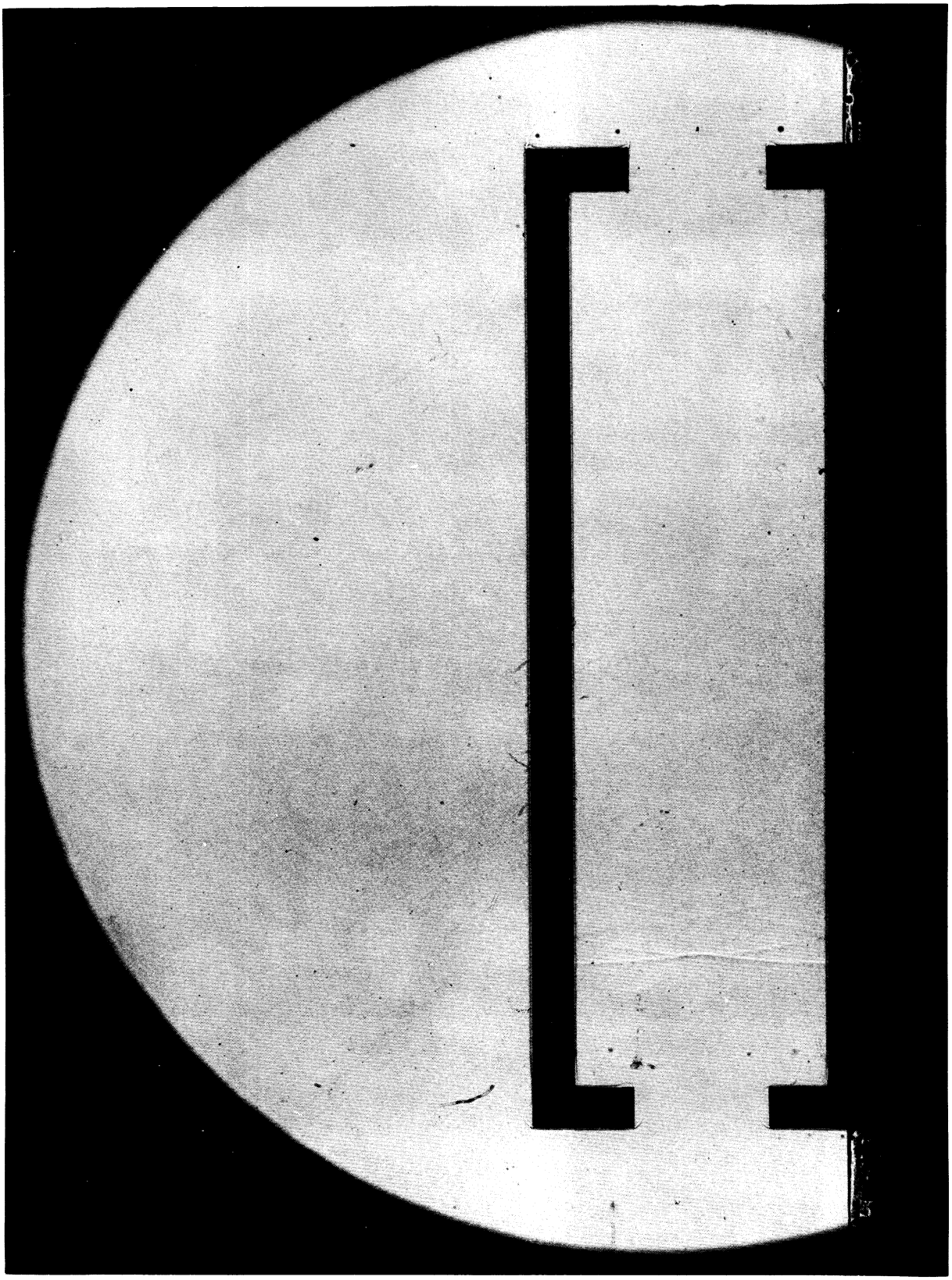

t = 577

Figure 5

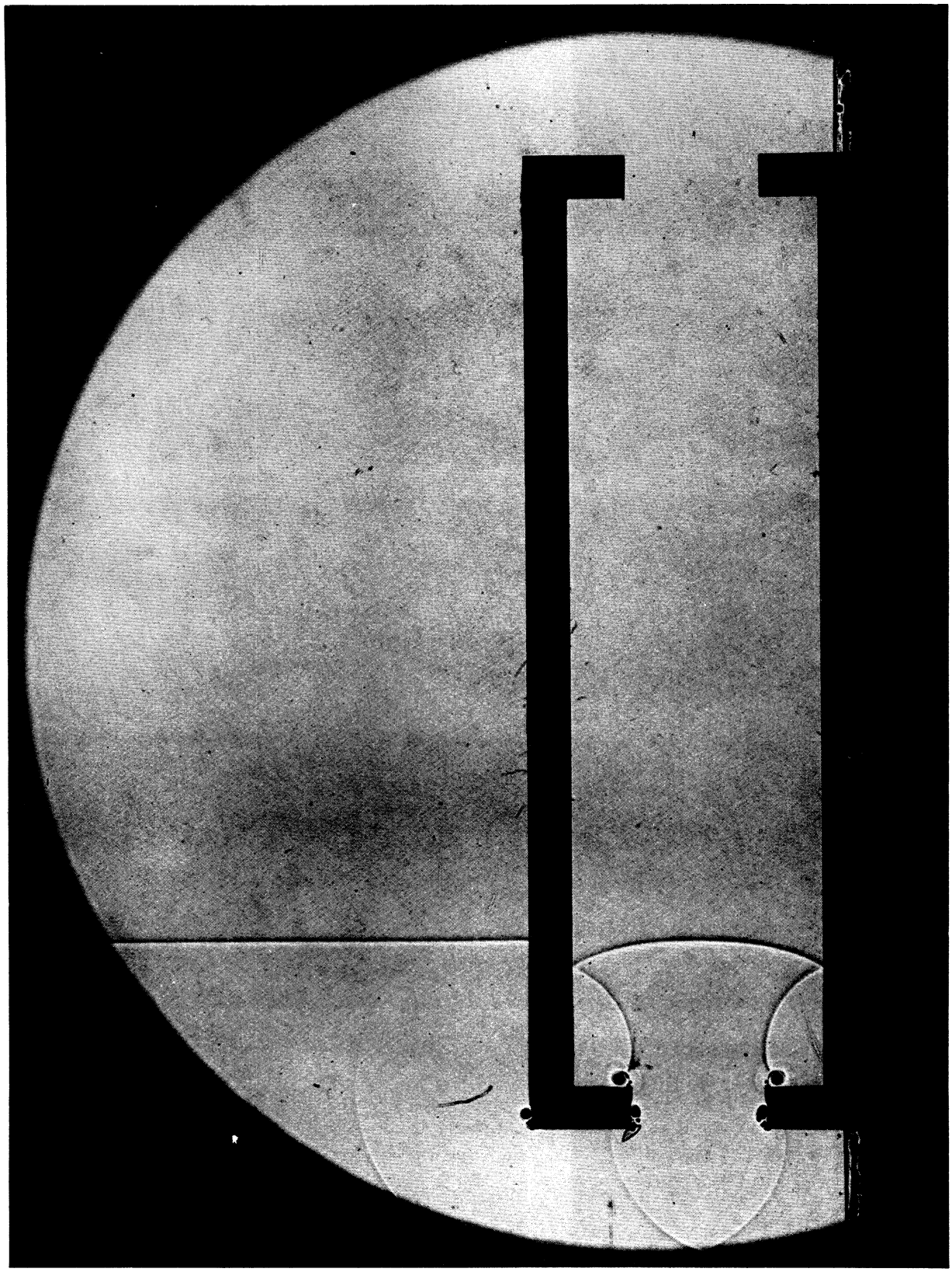

t = 54

Figure 6

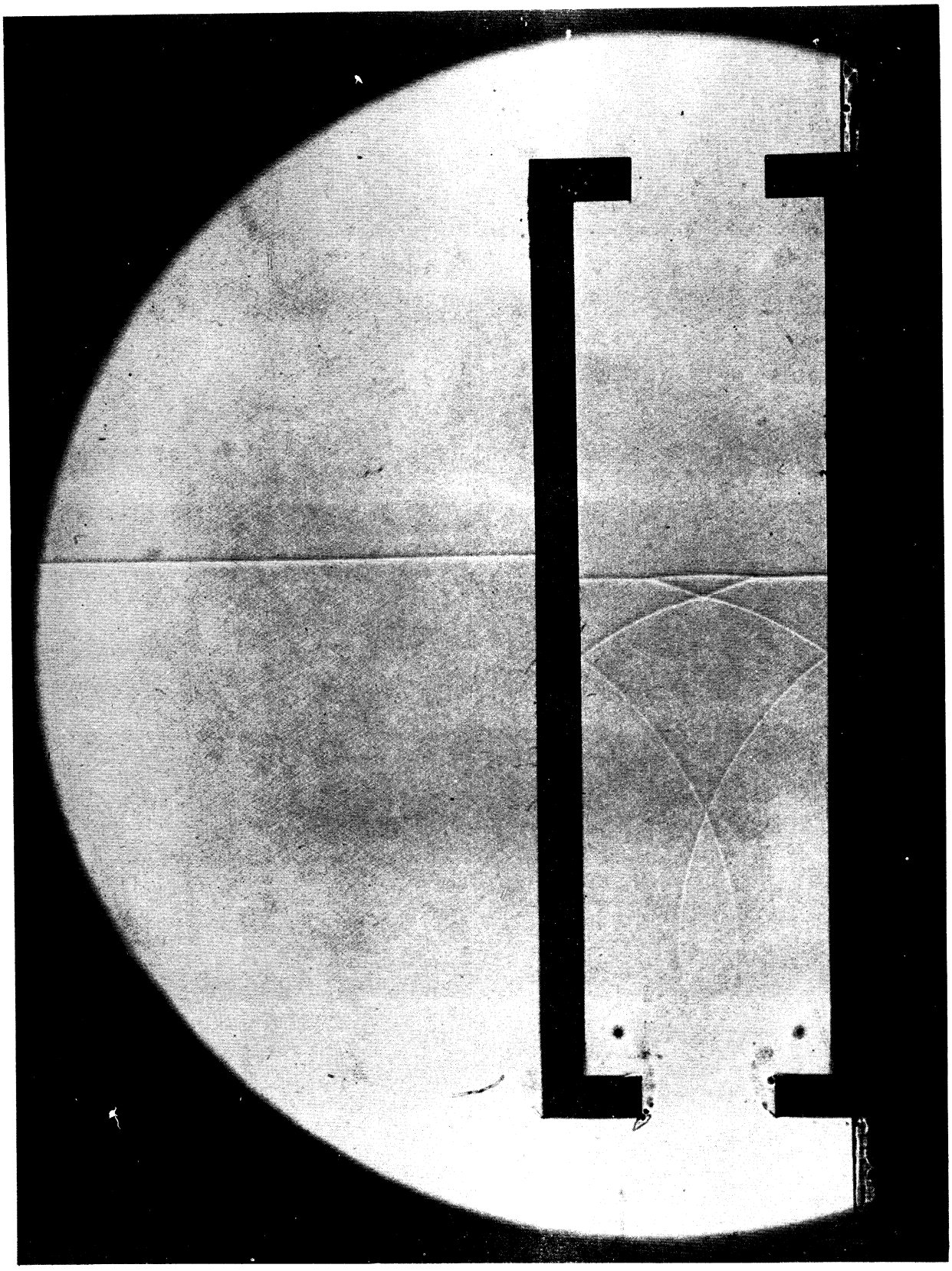

t = 166

Figure 7

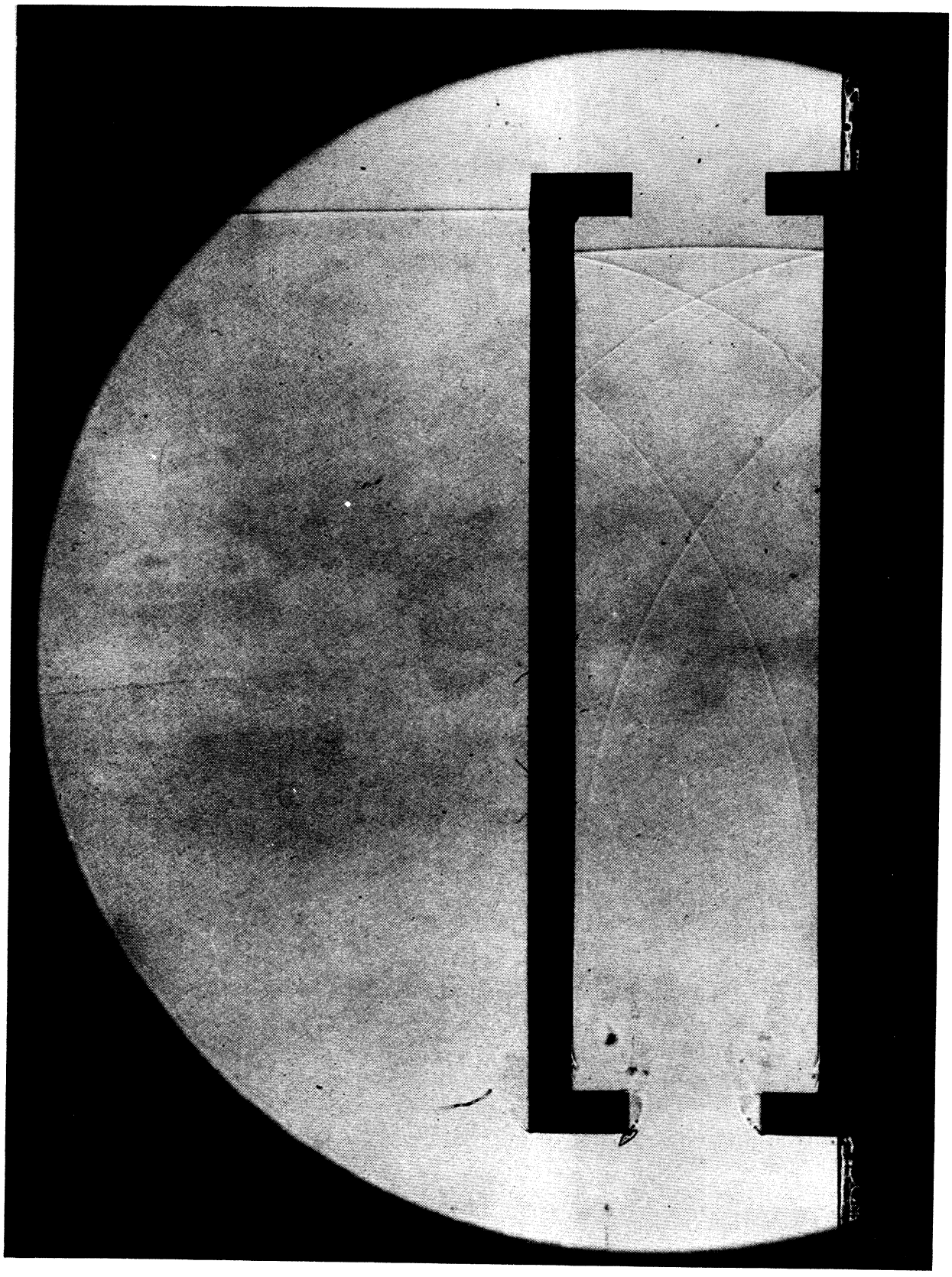

t = 271

Figure 8

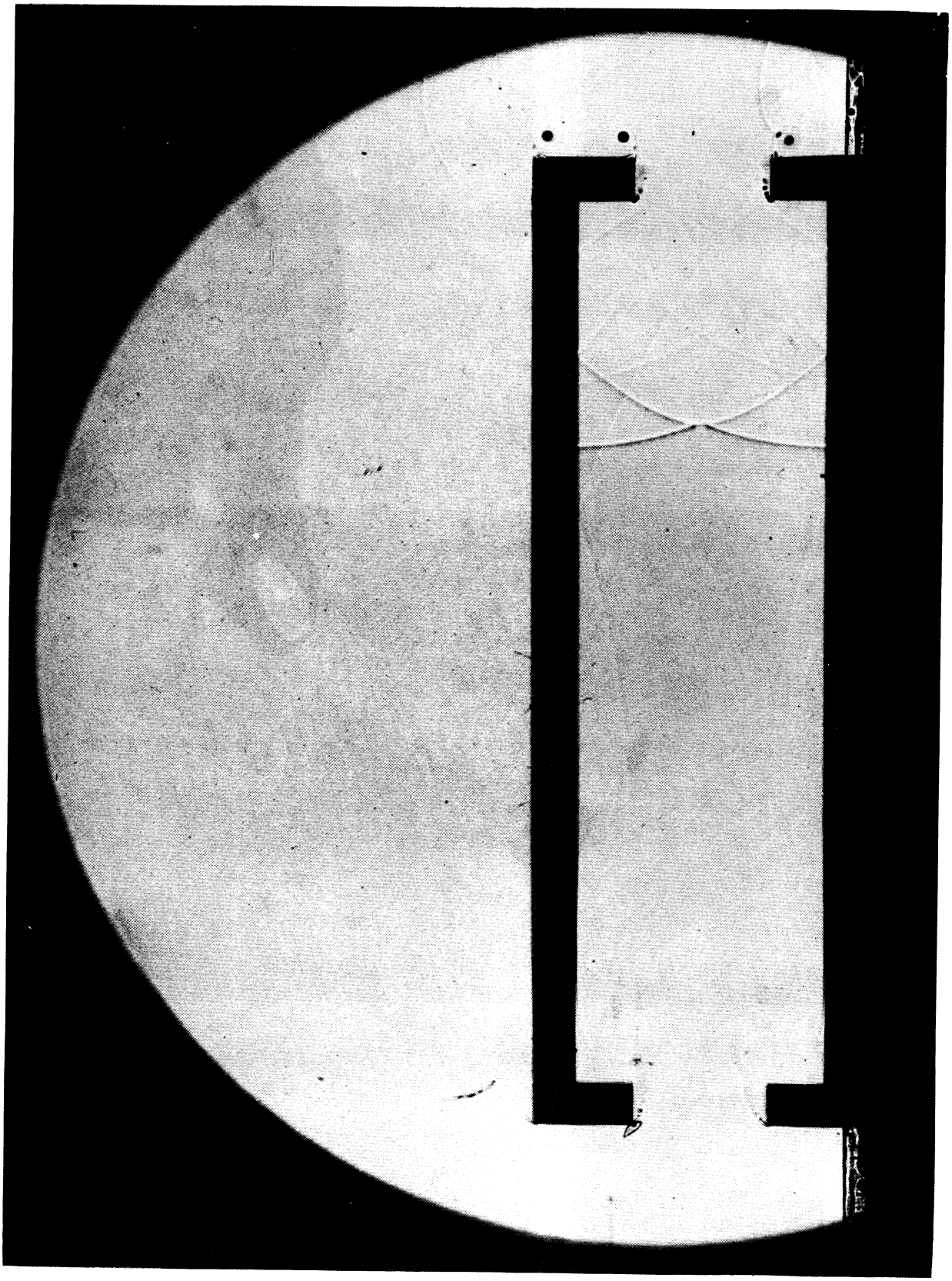

t = 370

Figure 9

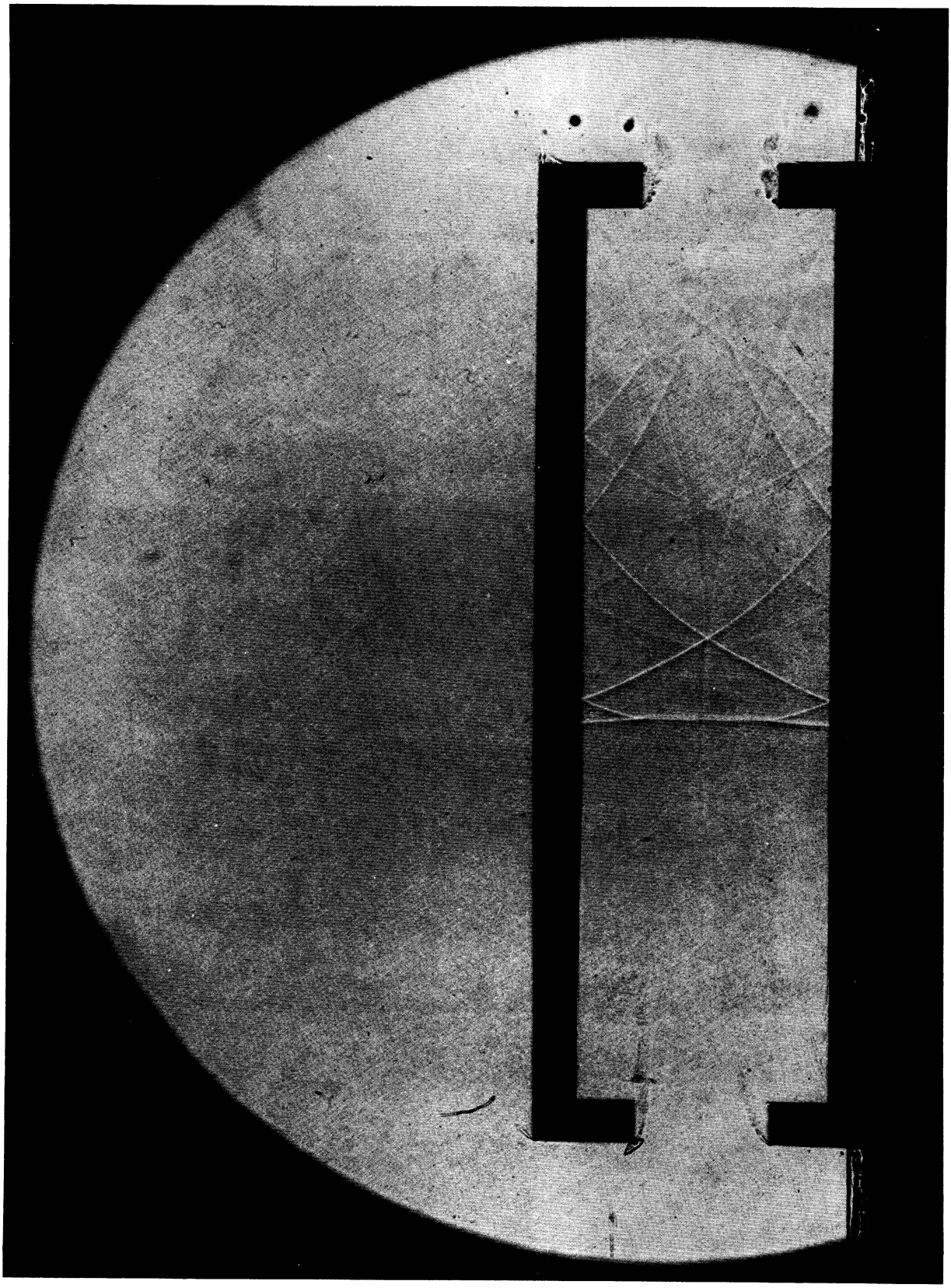

t = 476

Figure 10

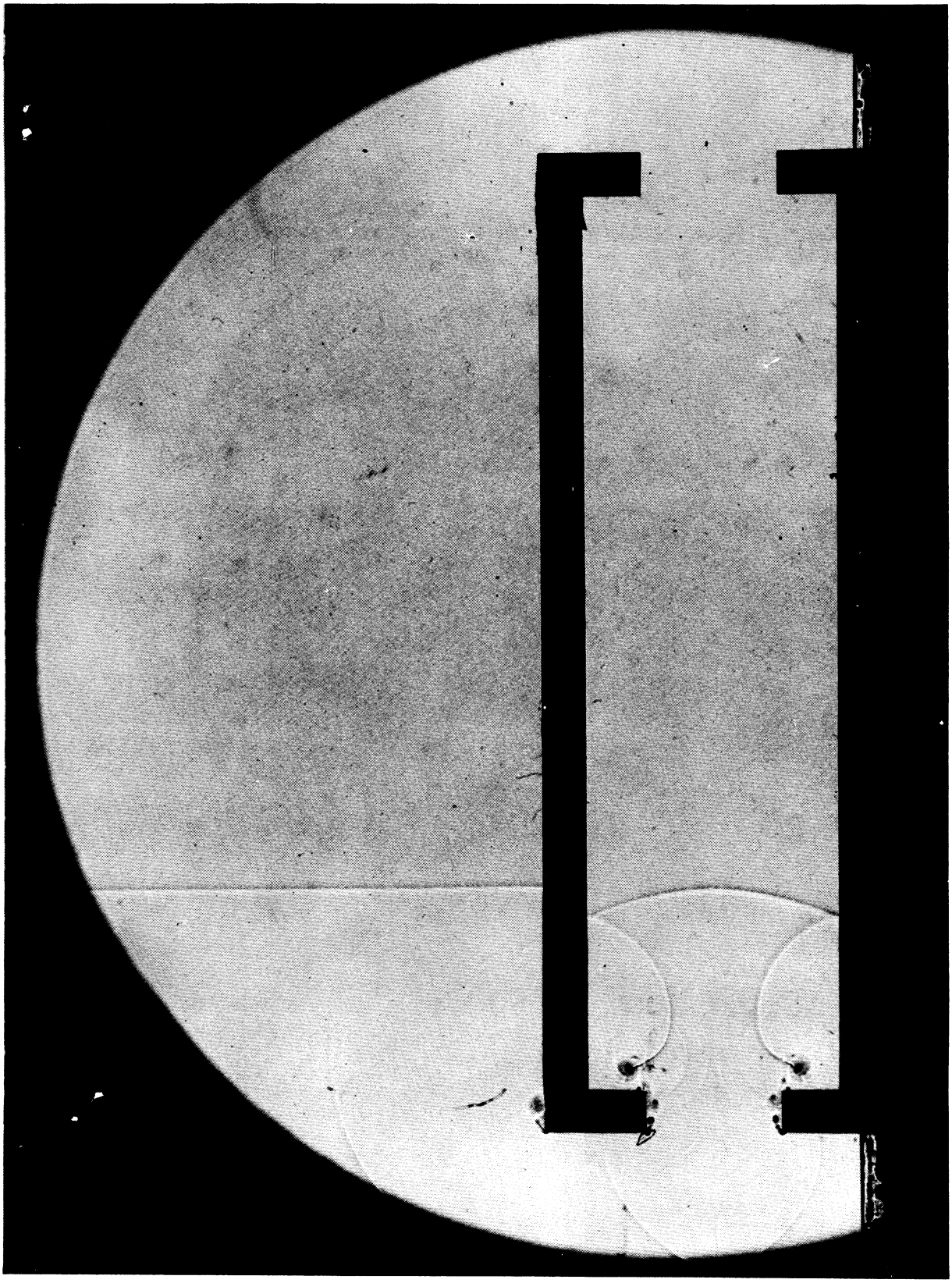

t = 64

Figure 11

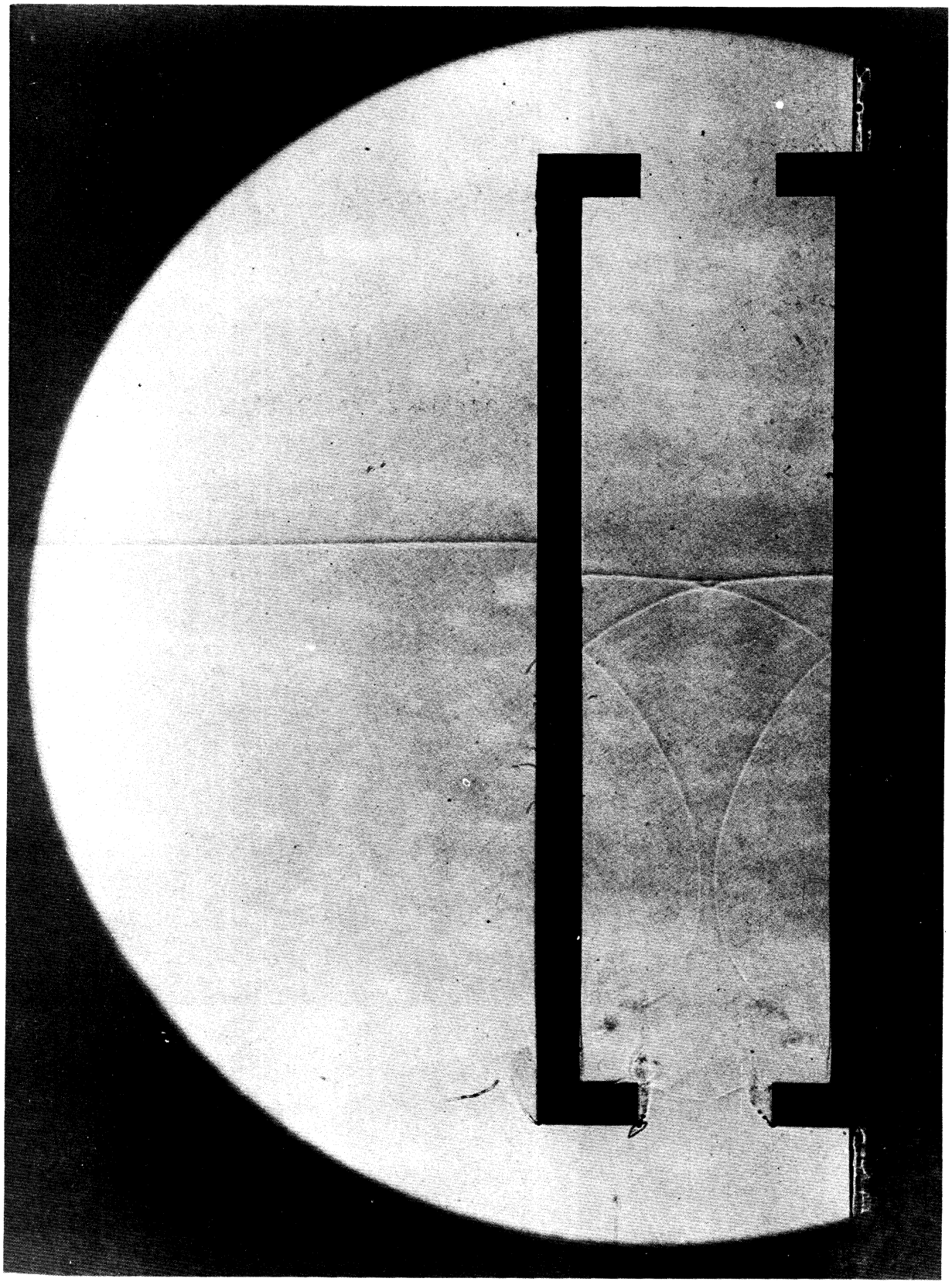

t = 153

Figure 12

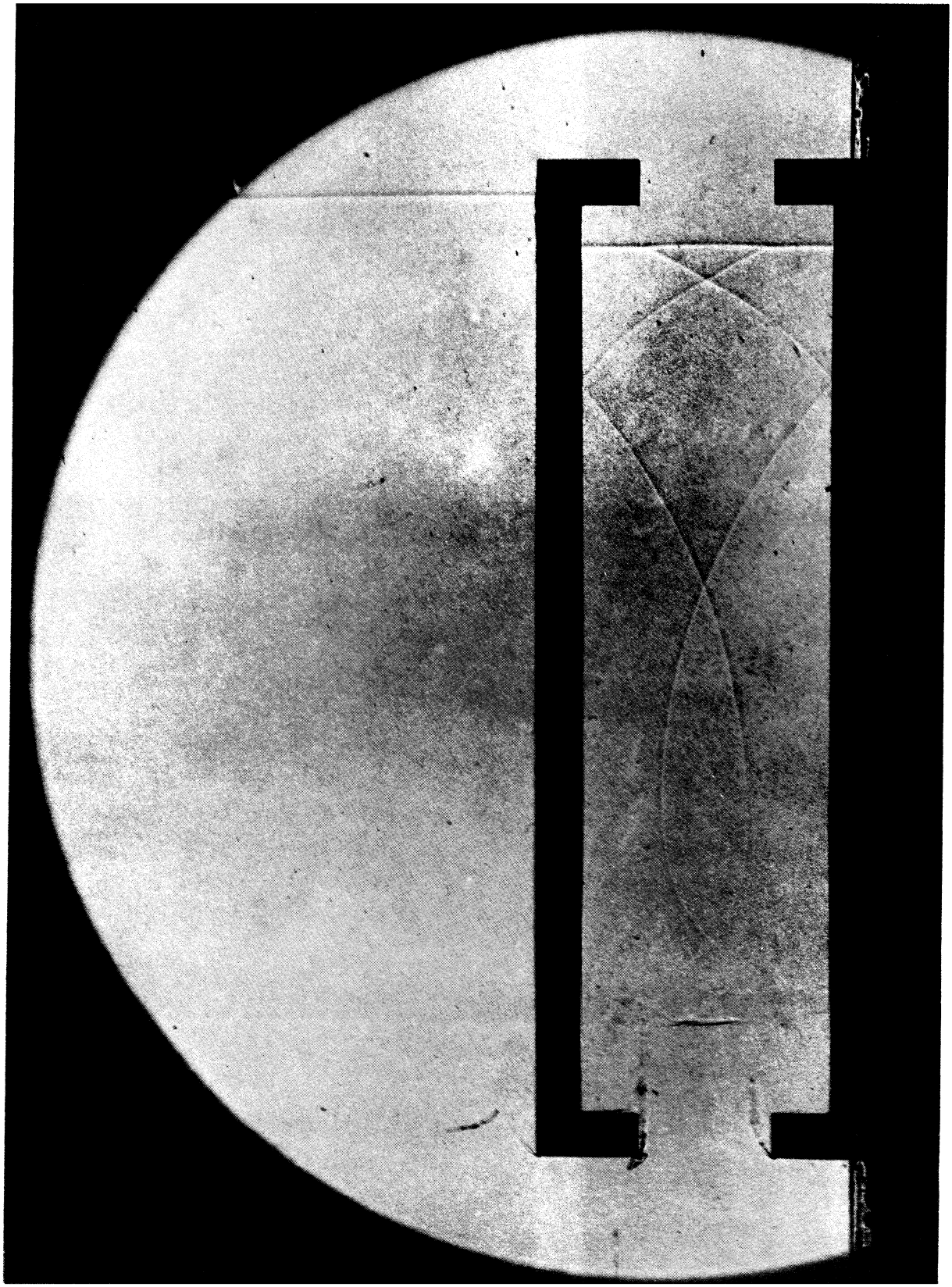

t = 246

Figure 13

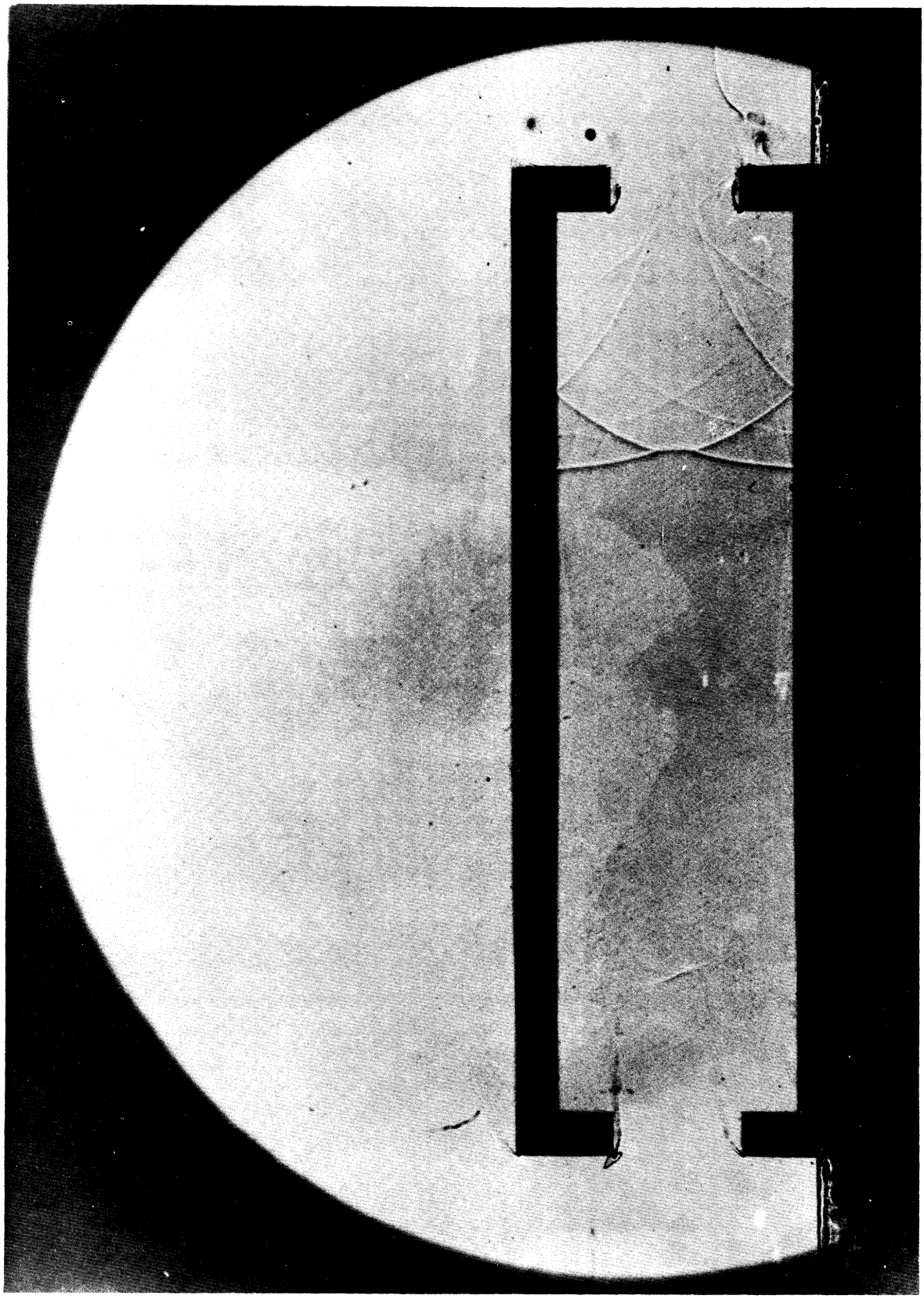

t = 353

Figure 14

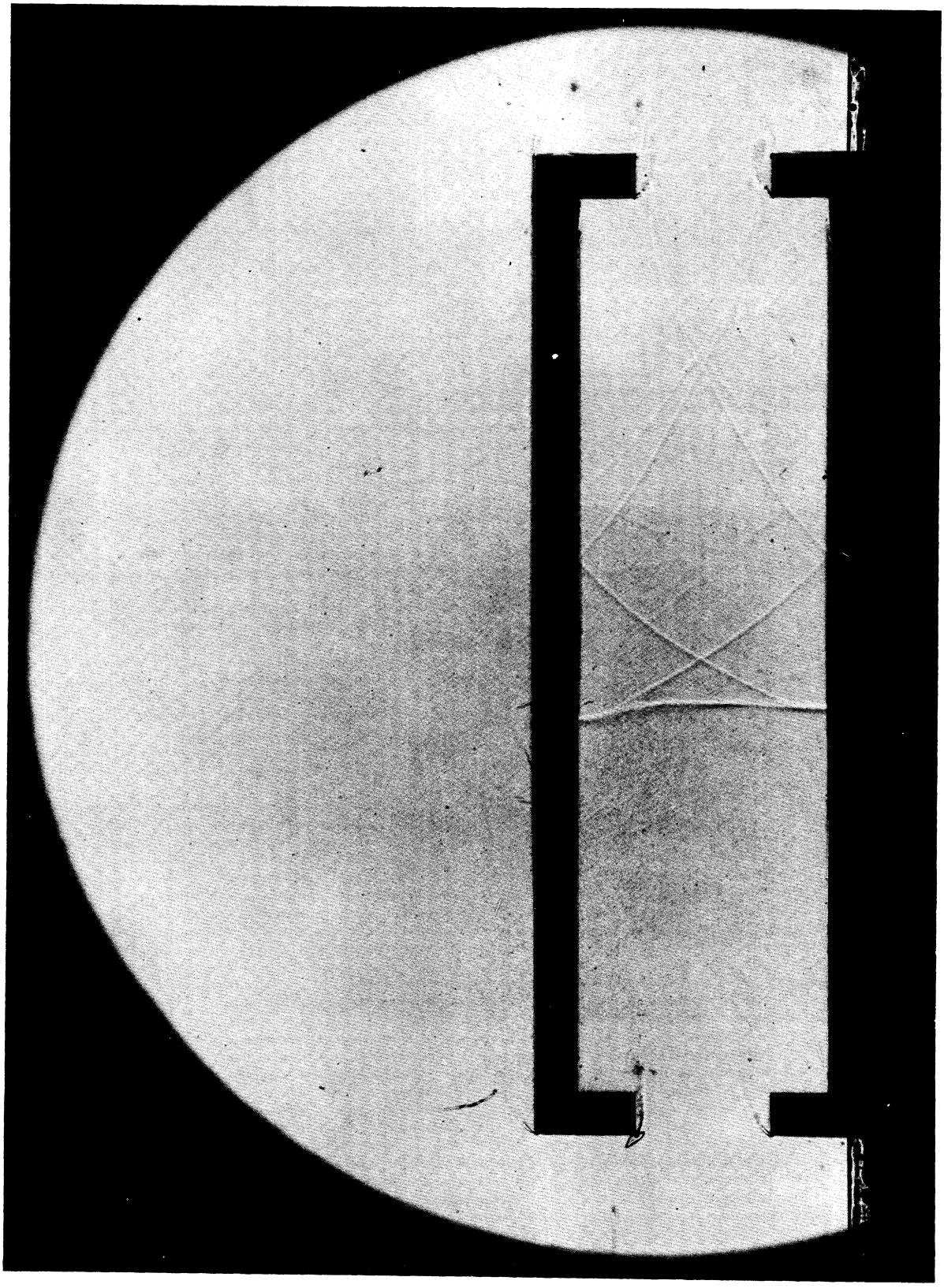

t = 463

Figure 15

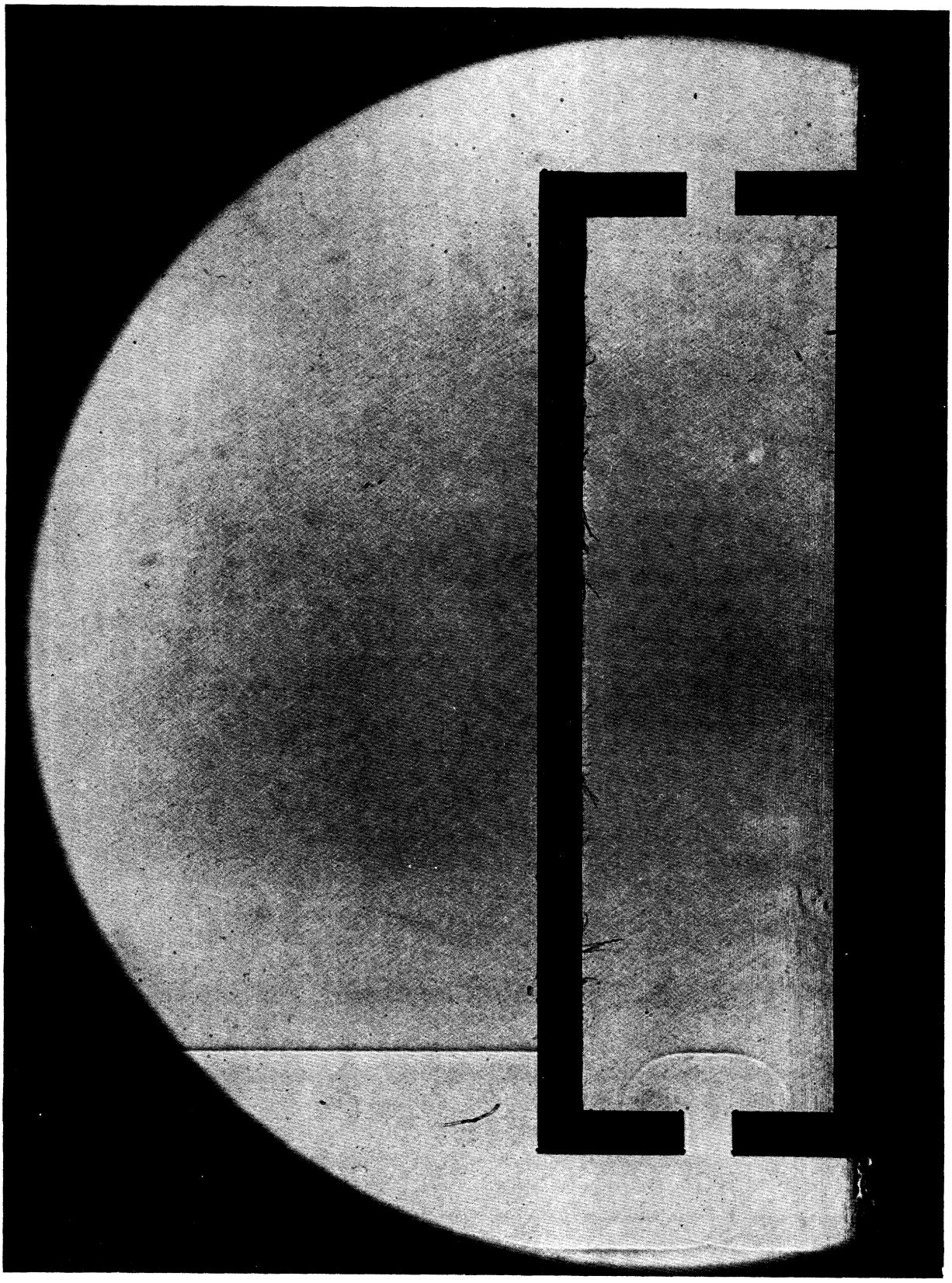

t = 33

Figure 16

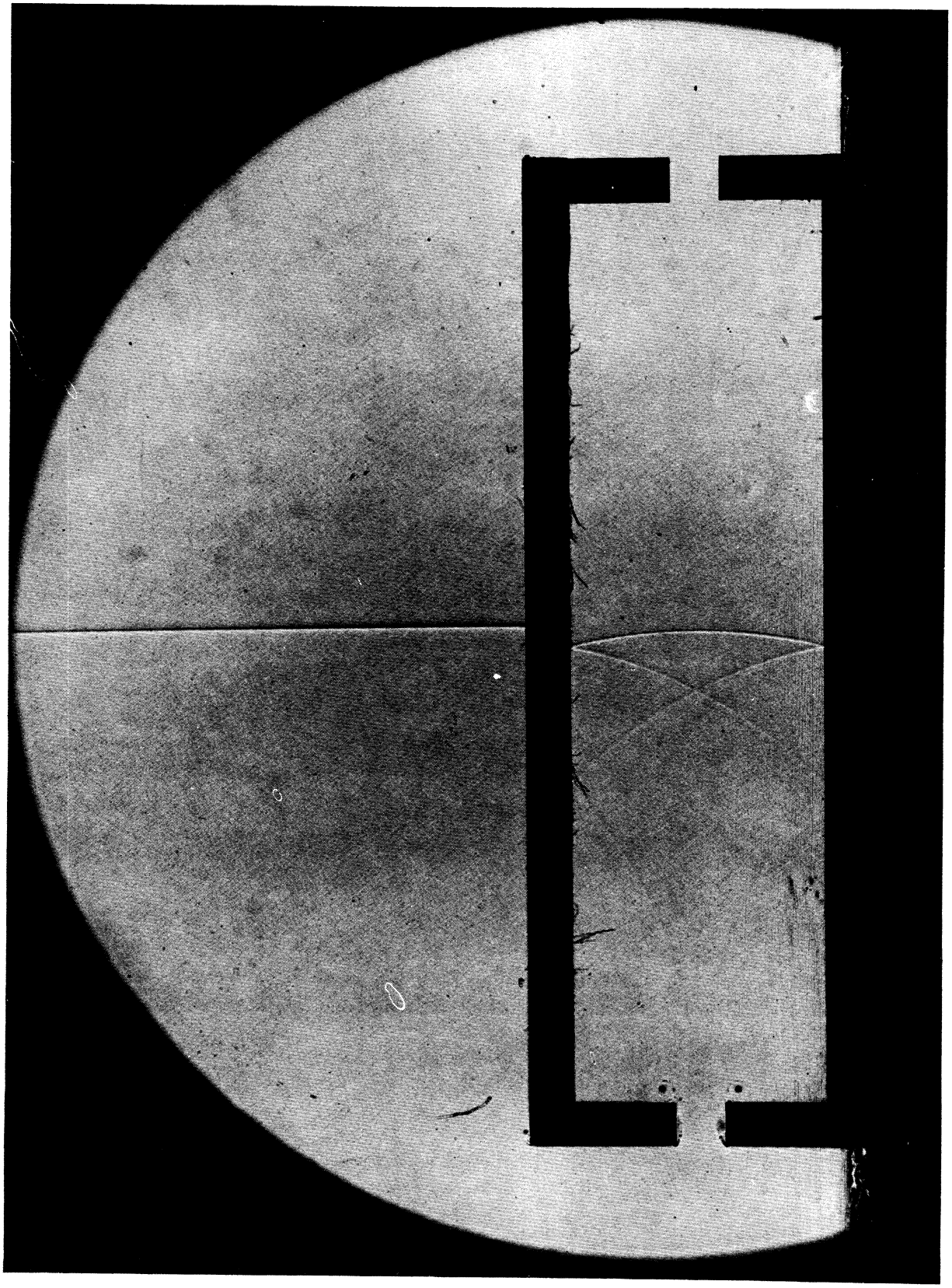

t = 168

Figure 17

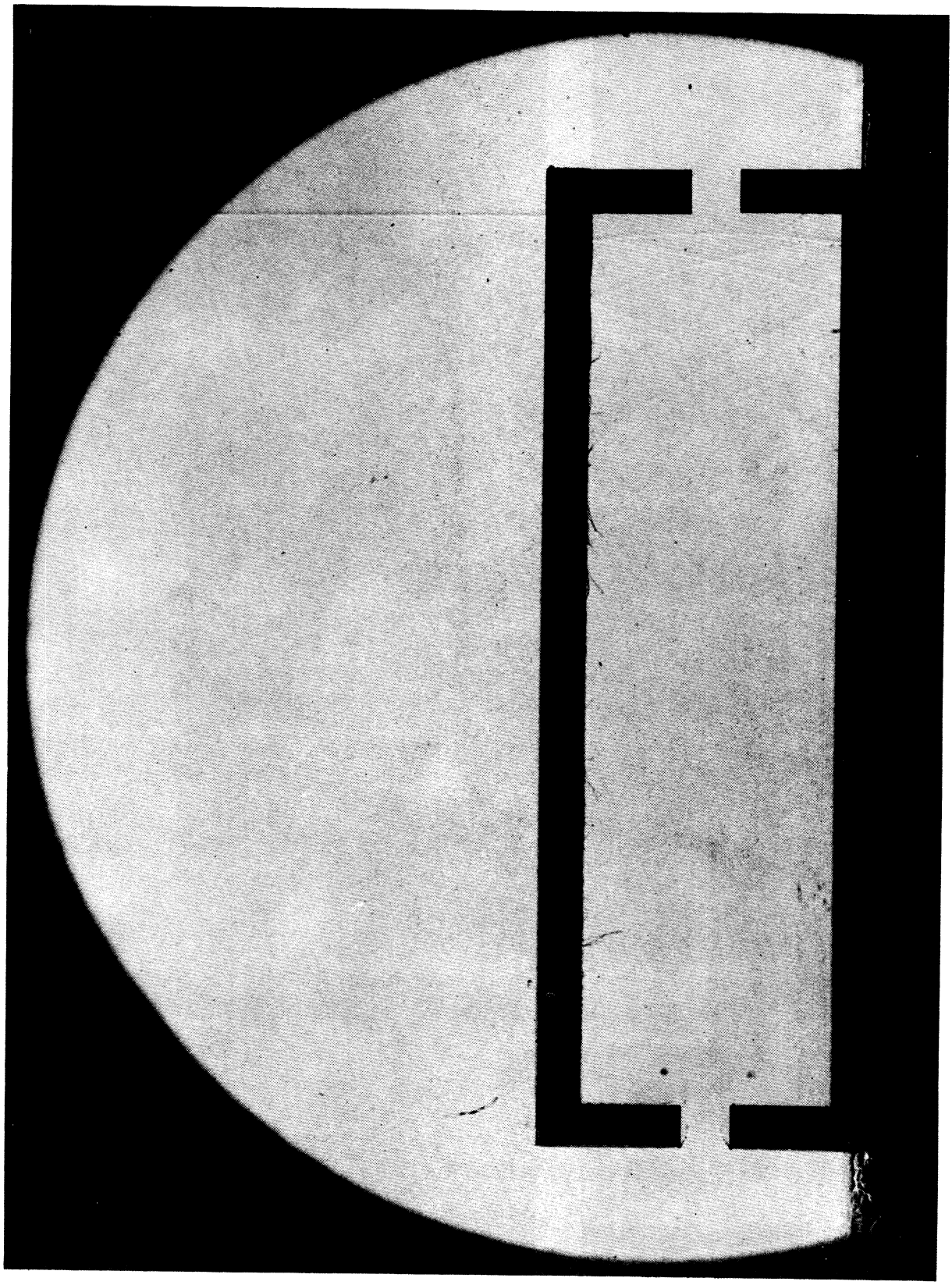

t = 302

Figure 18

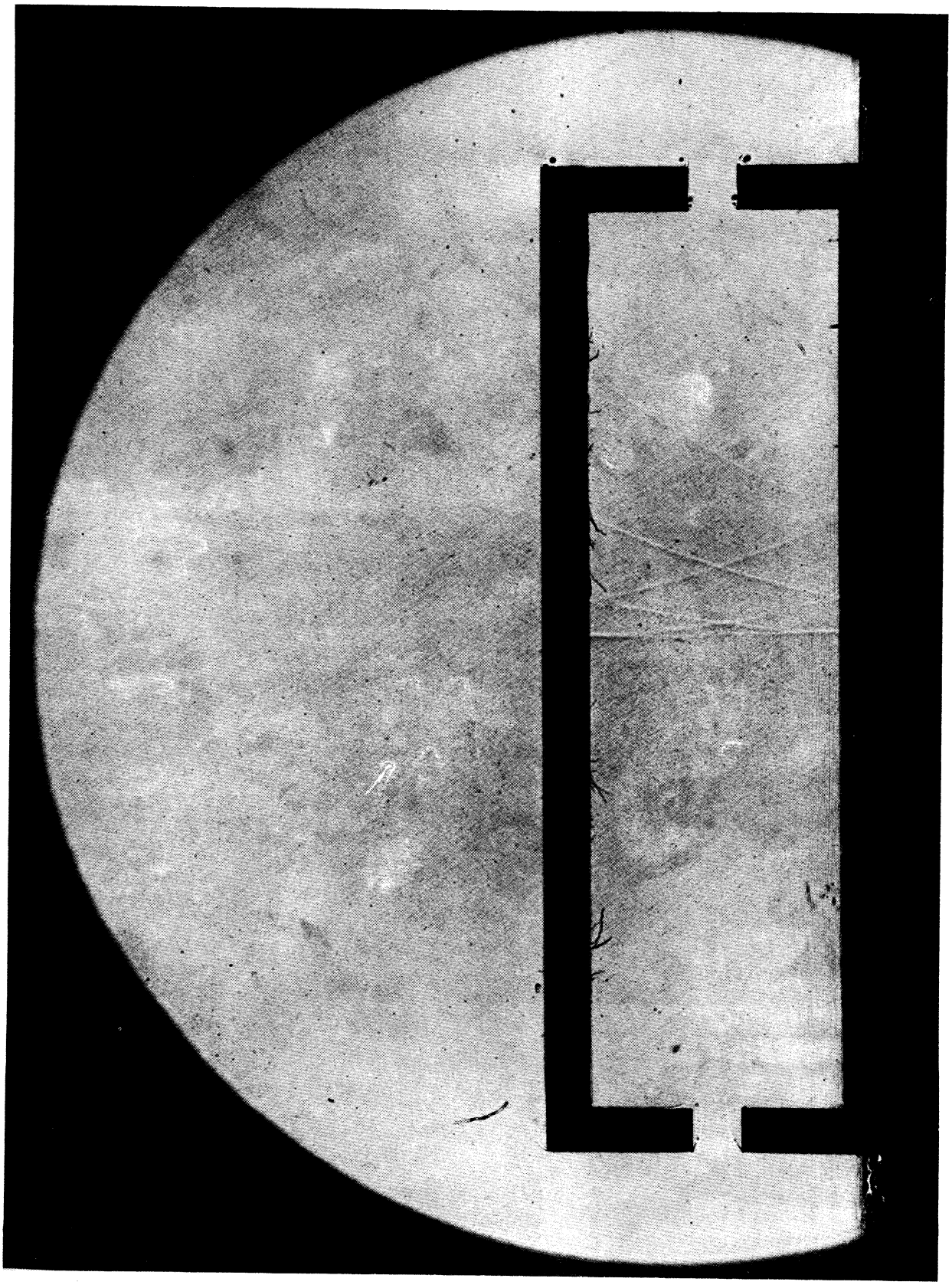

t = 458

Figure 19

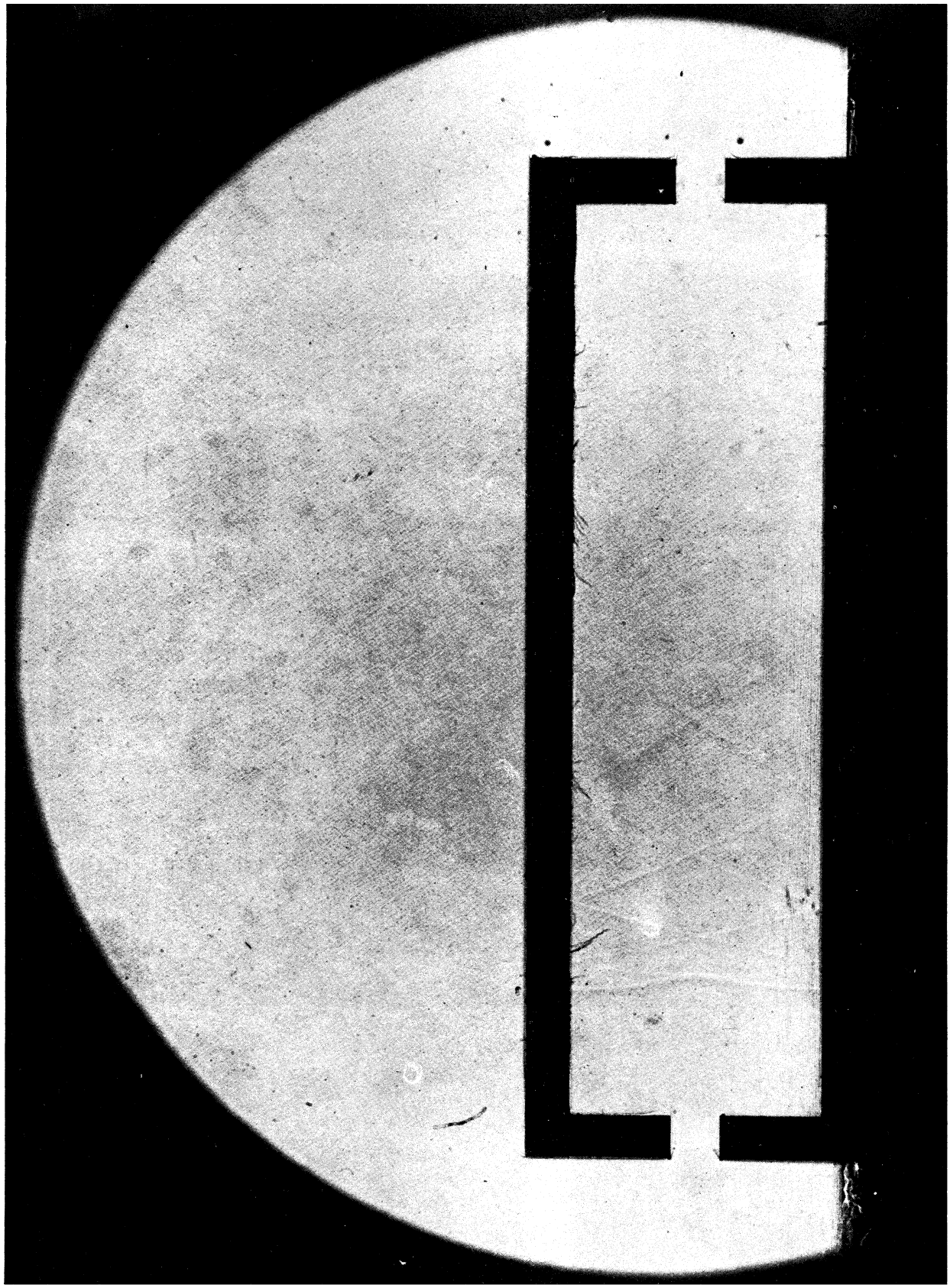

t = 576

Figure 20

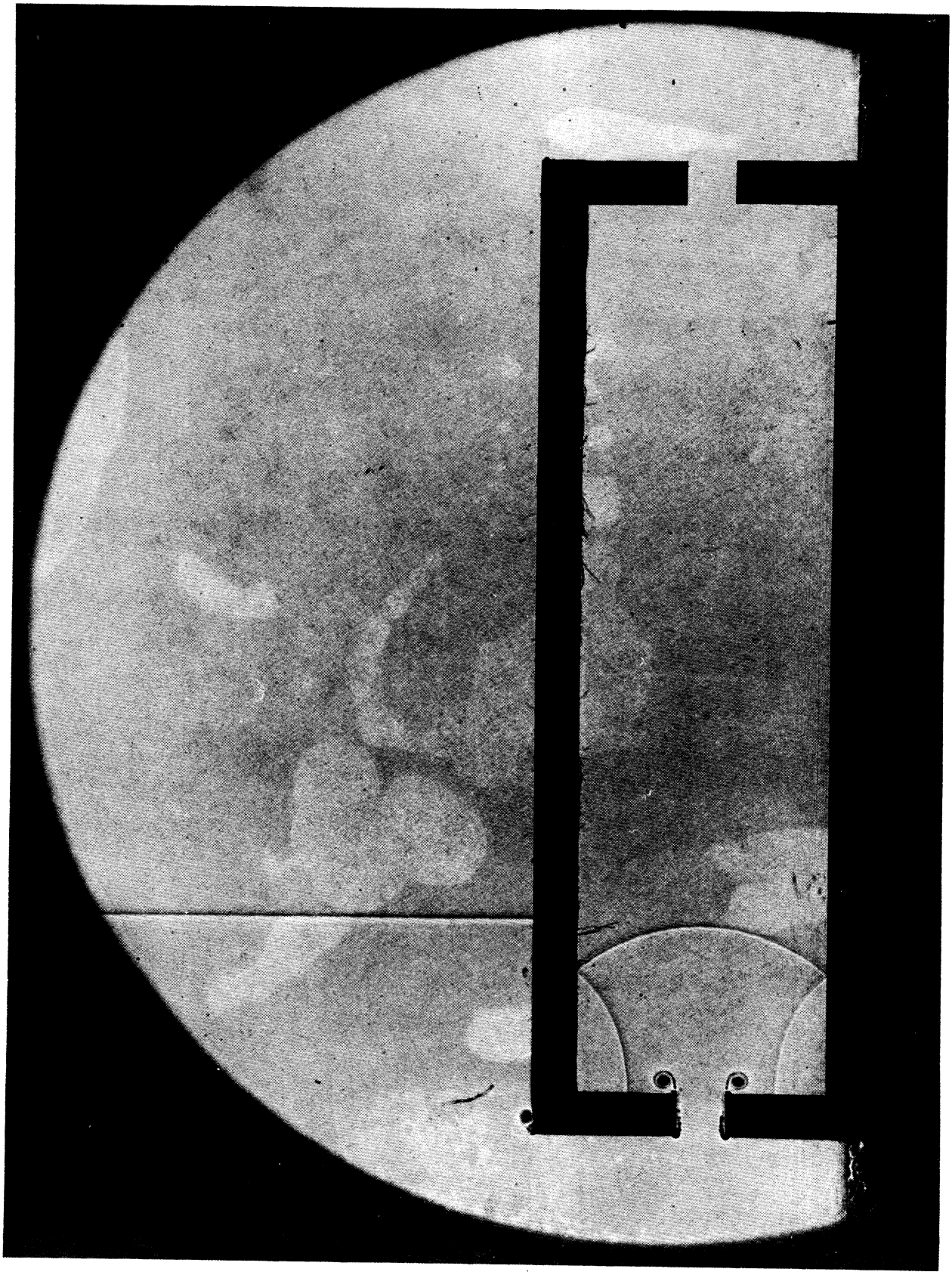

t = 63

Figure 21

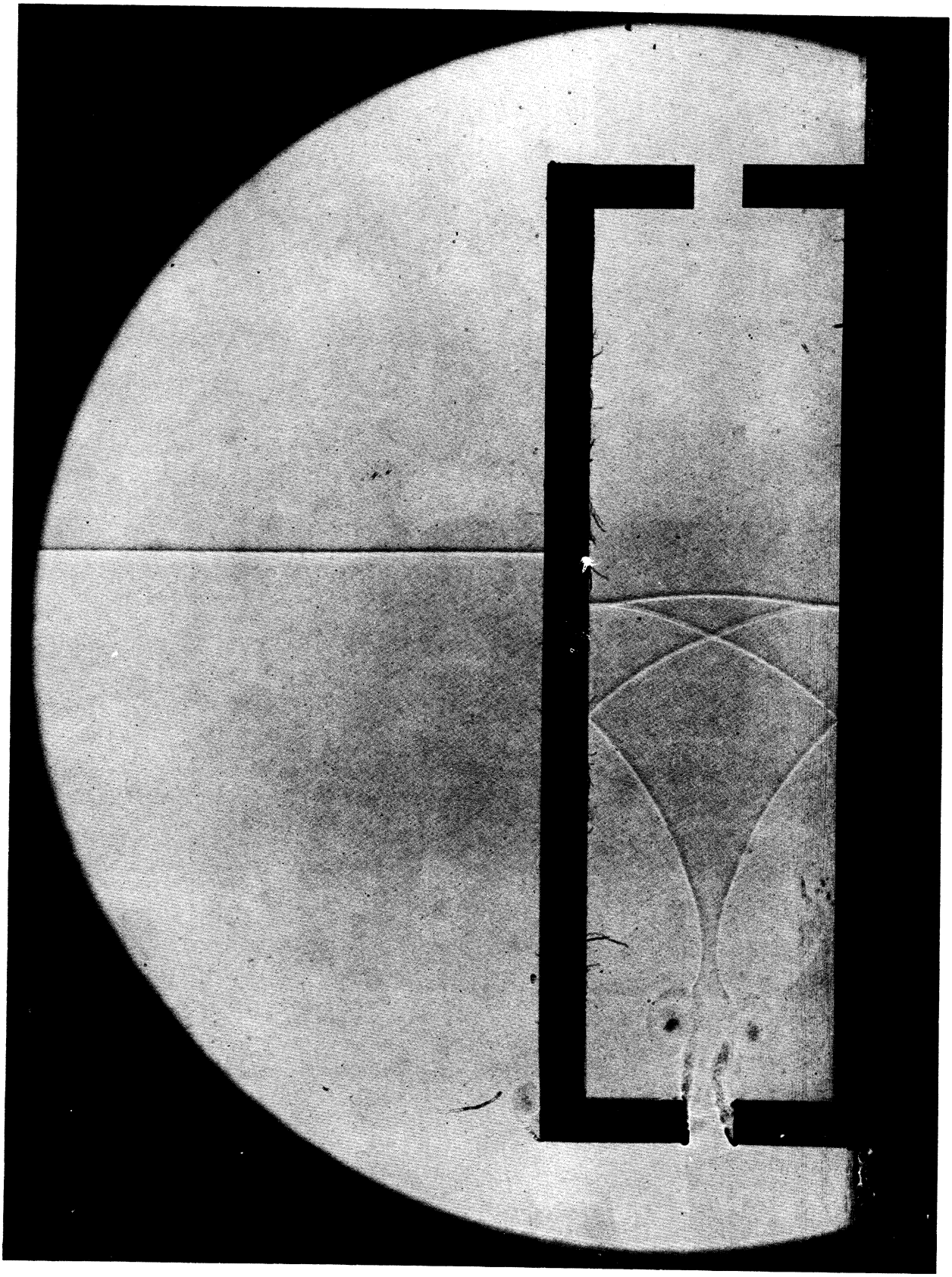

t = 167

Figure 22

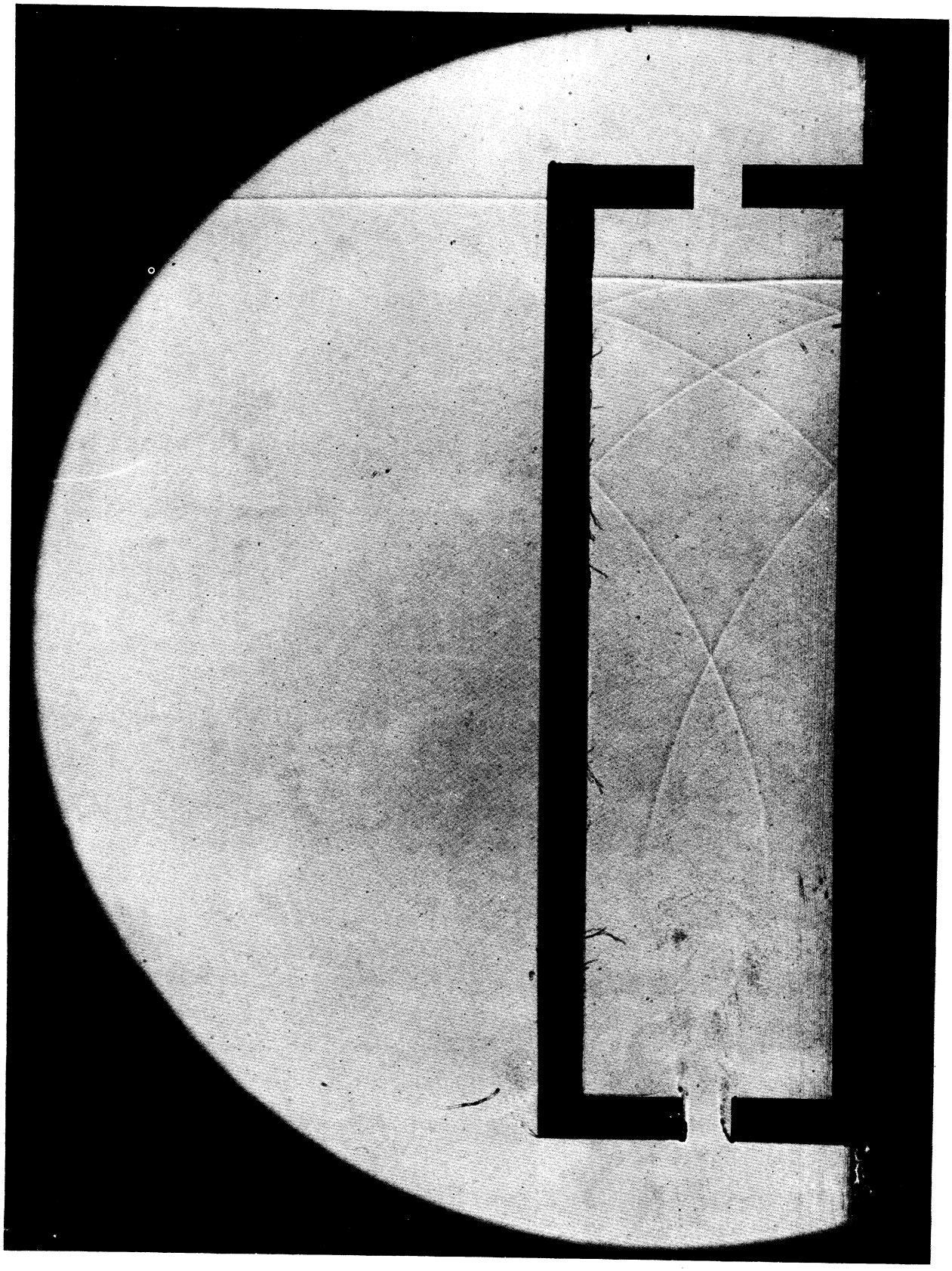

t = 271

Figure 23

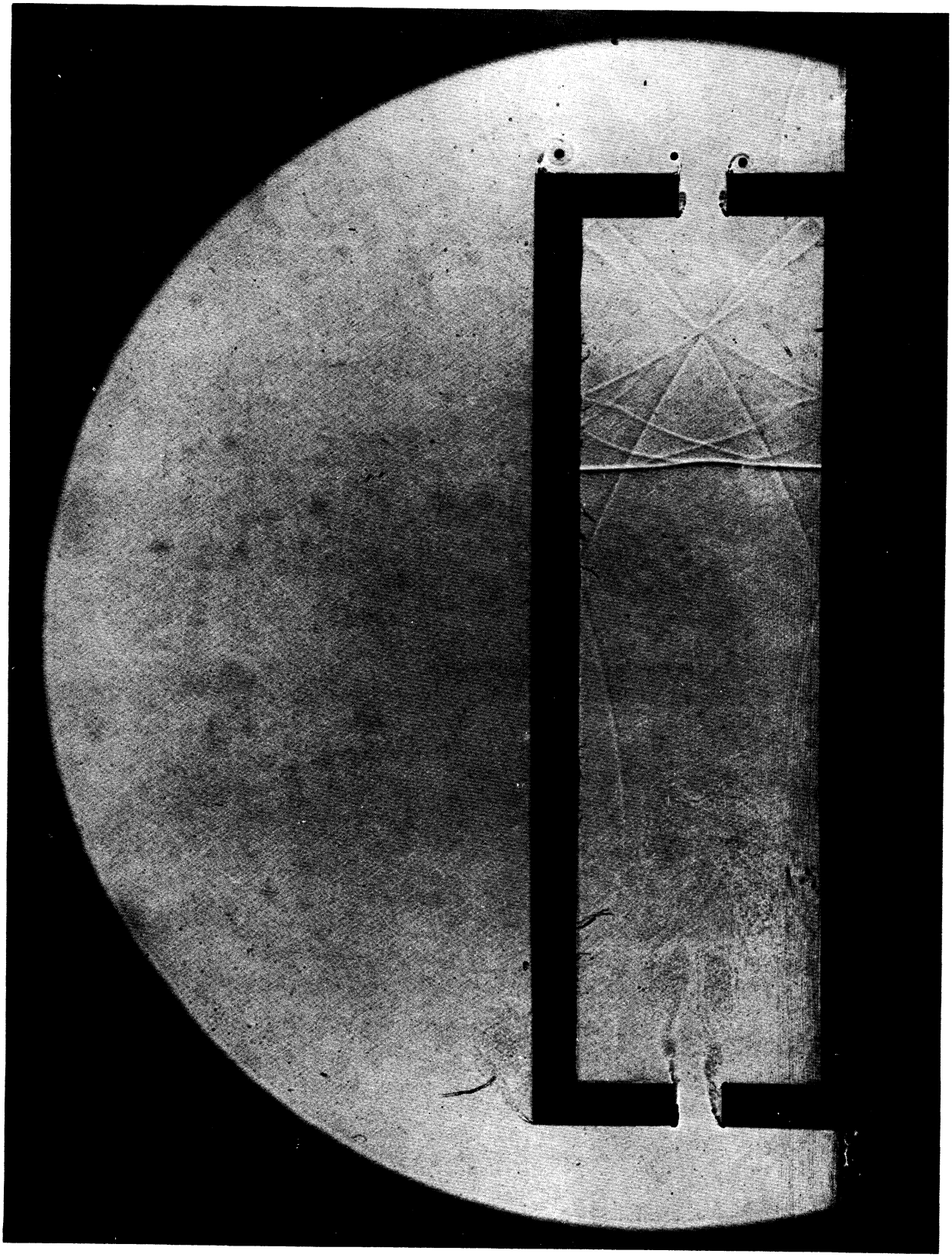

t = 389

Figure 24

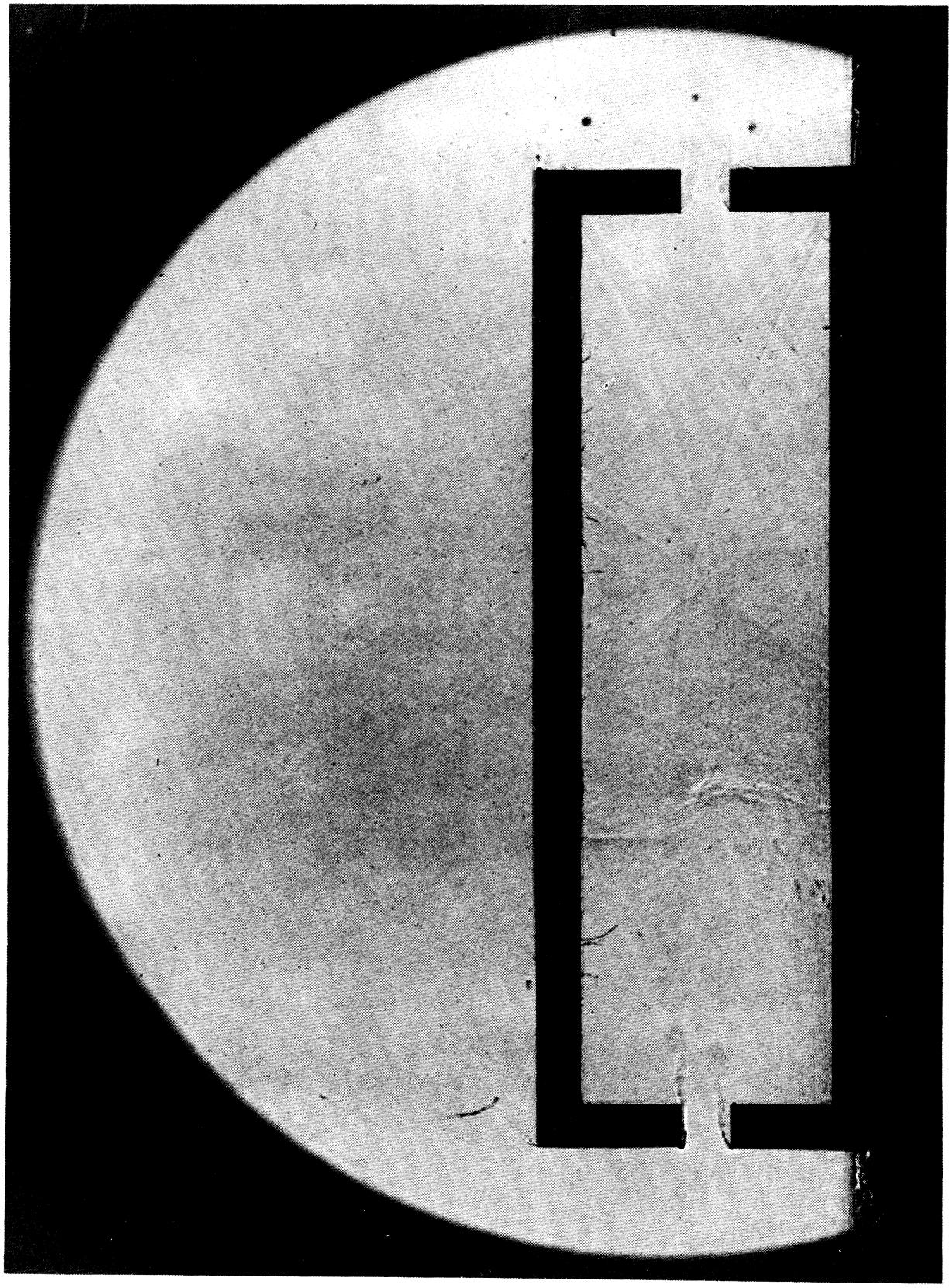

t = 504

Figure 25

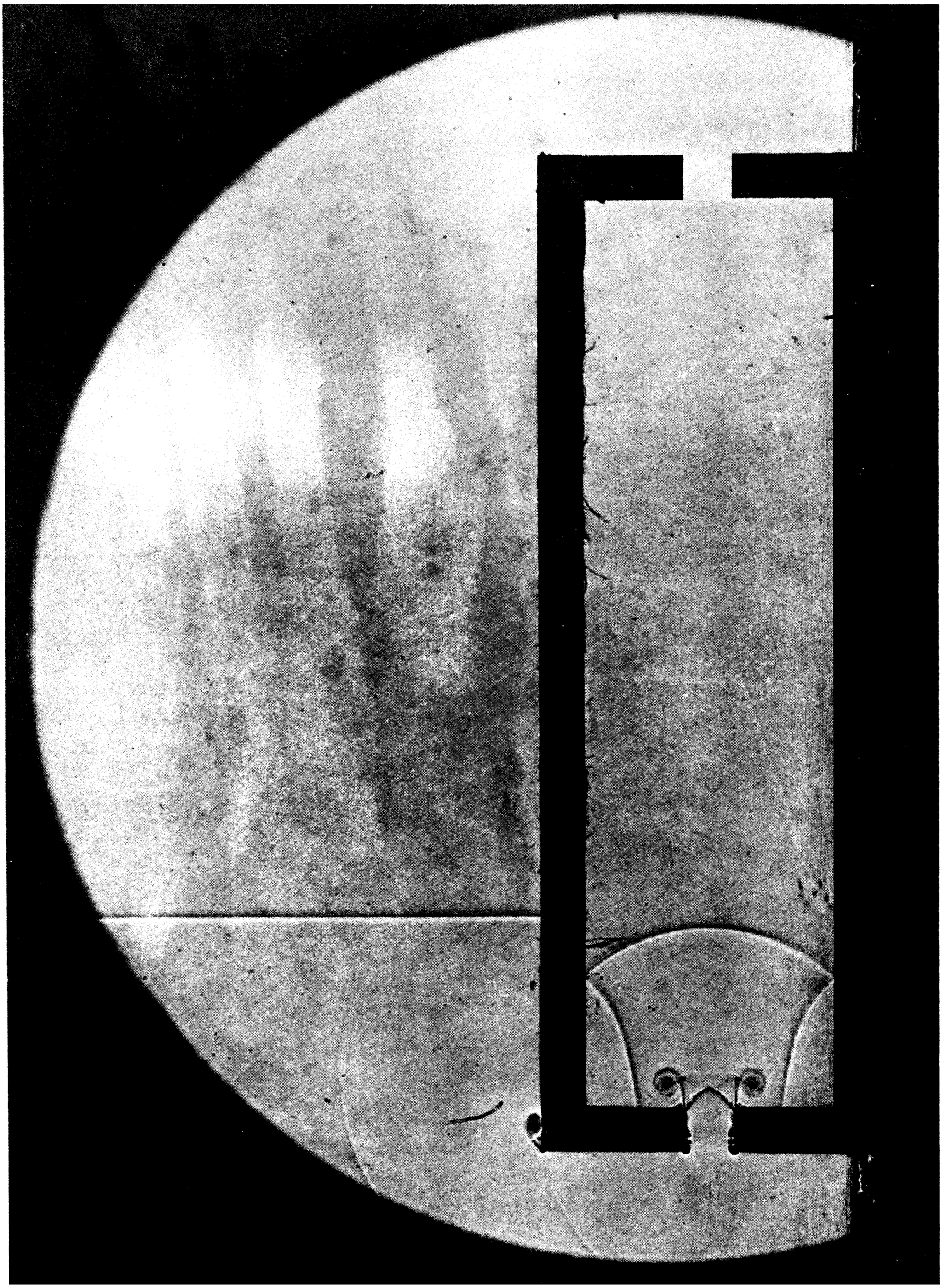

t = 60

Figure 26

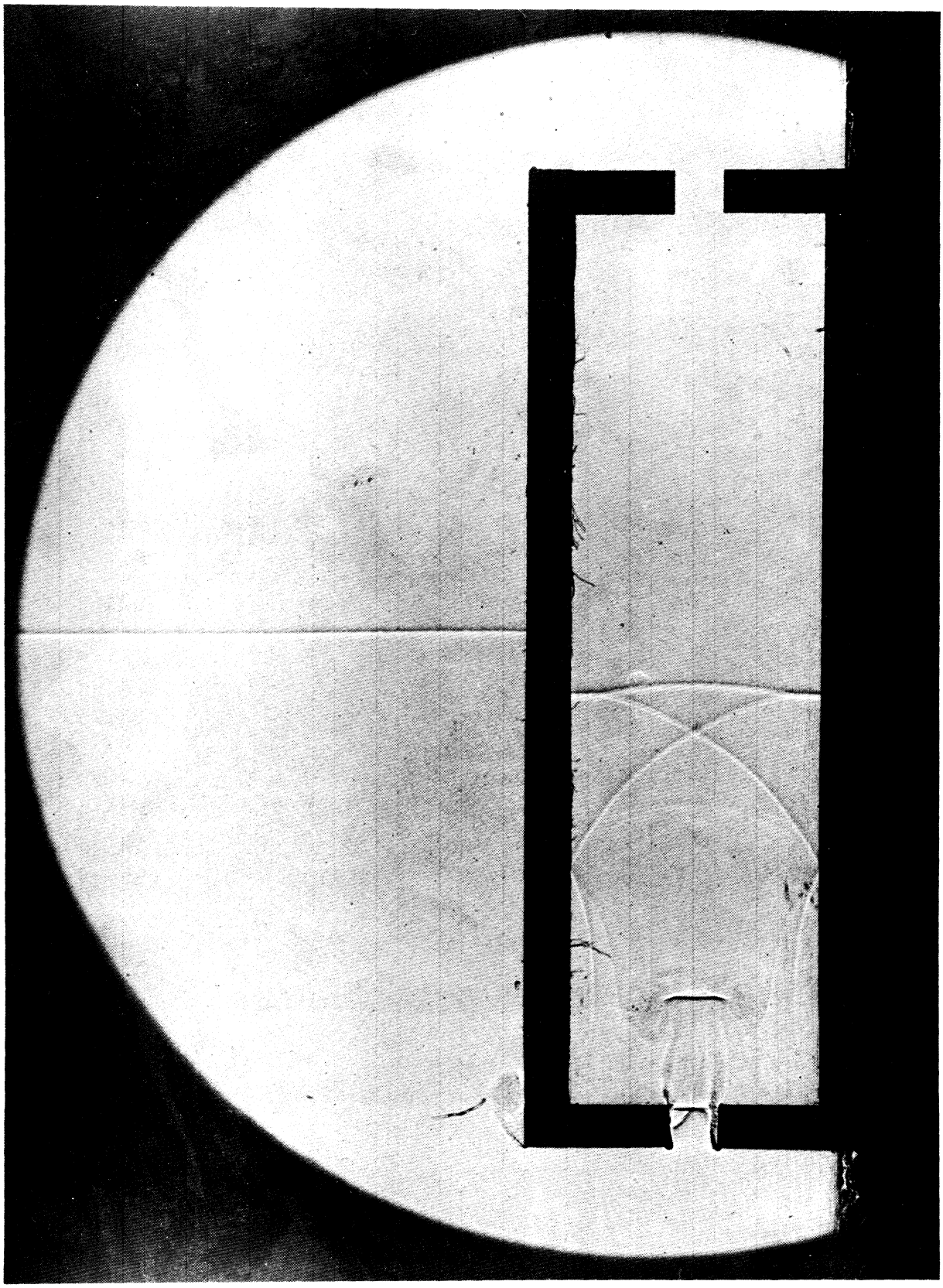

t = 136

Figure 27

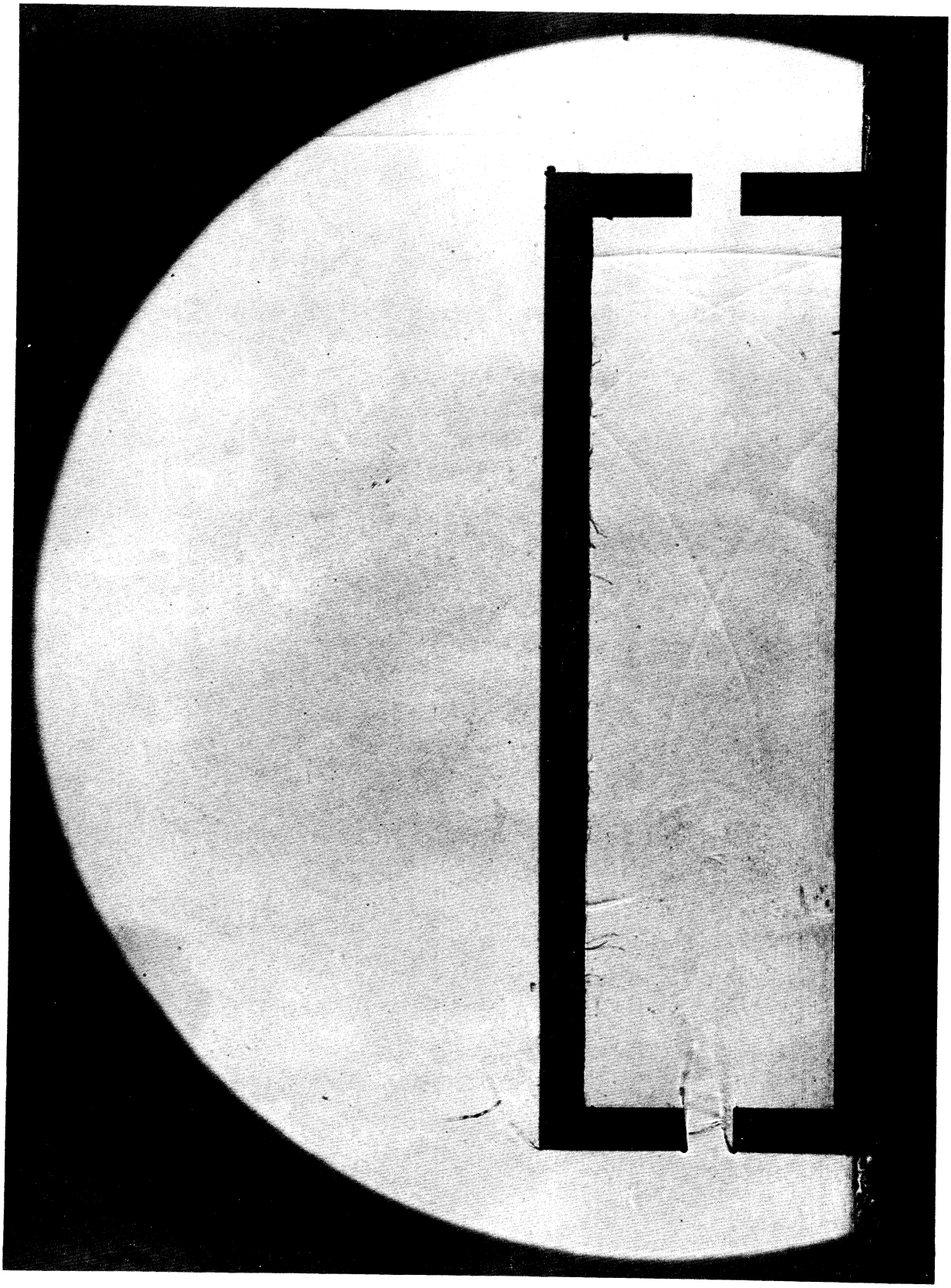

t = 262

Figure 28

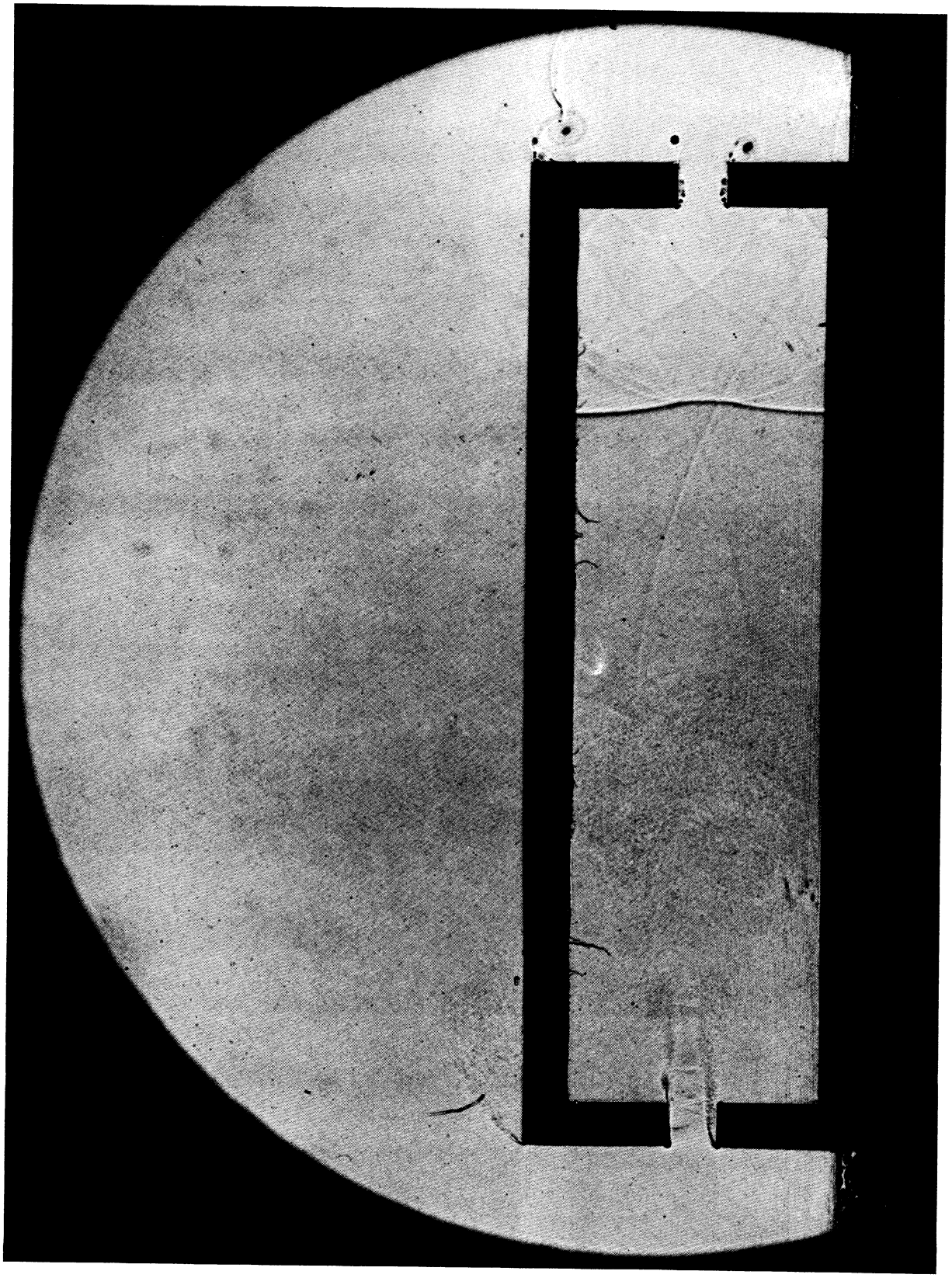

t = 343

Figure 29

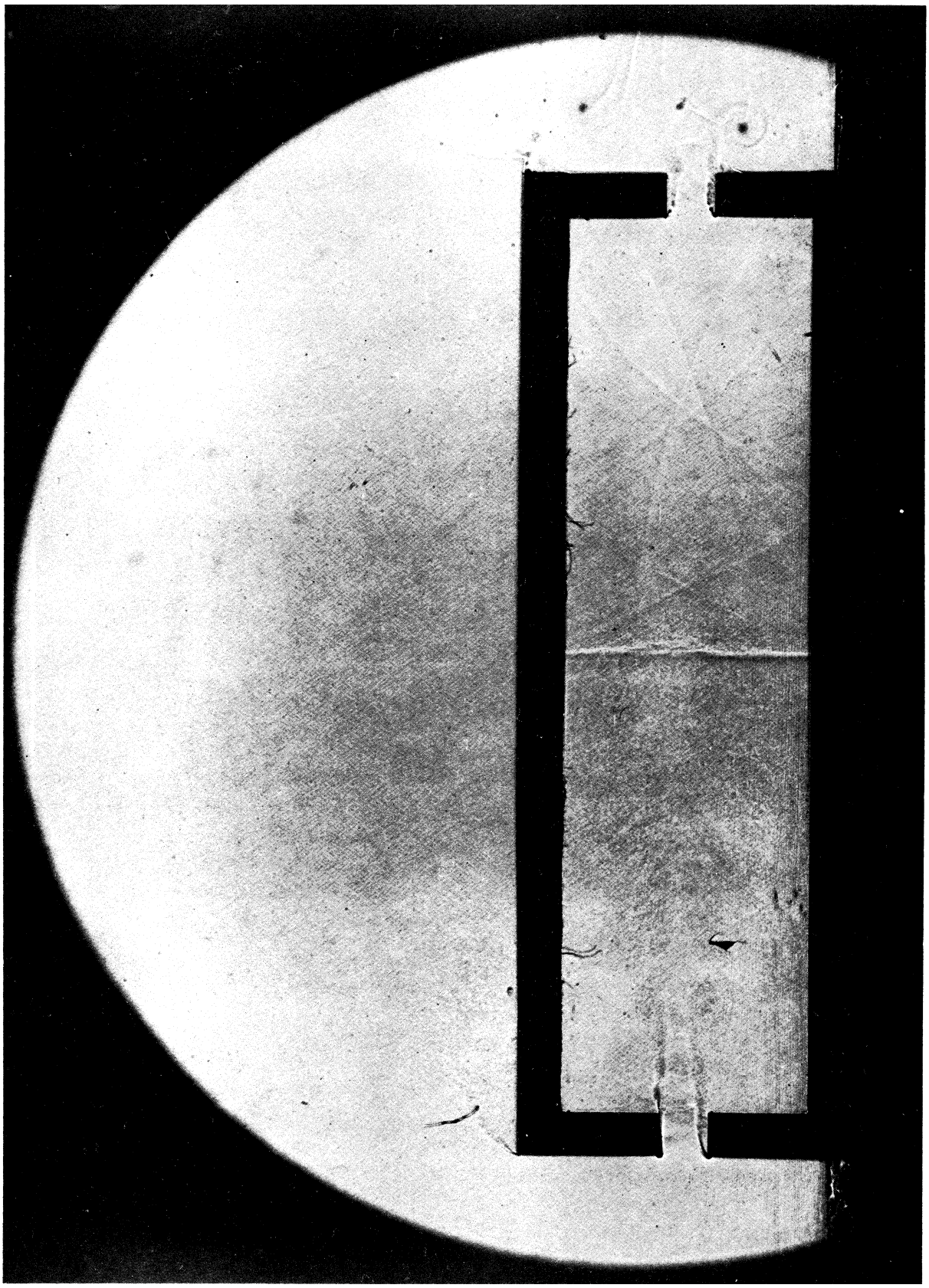

t = 423

Figure 30

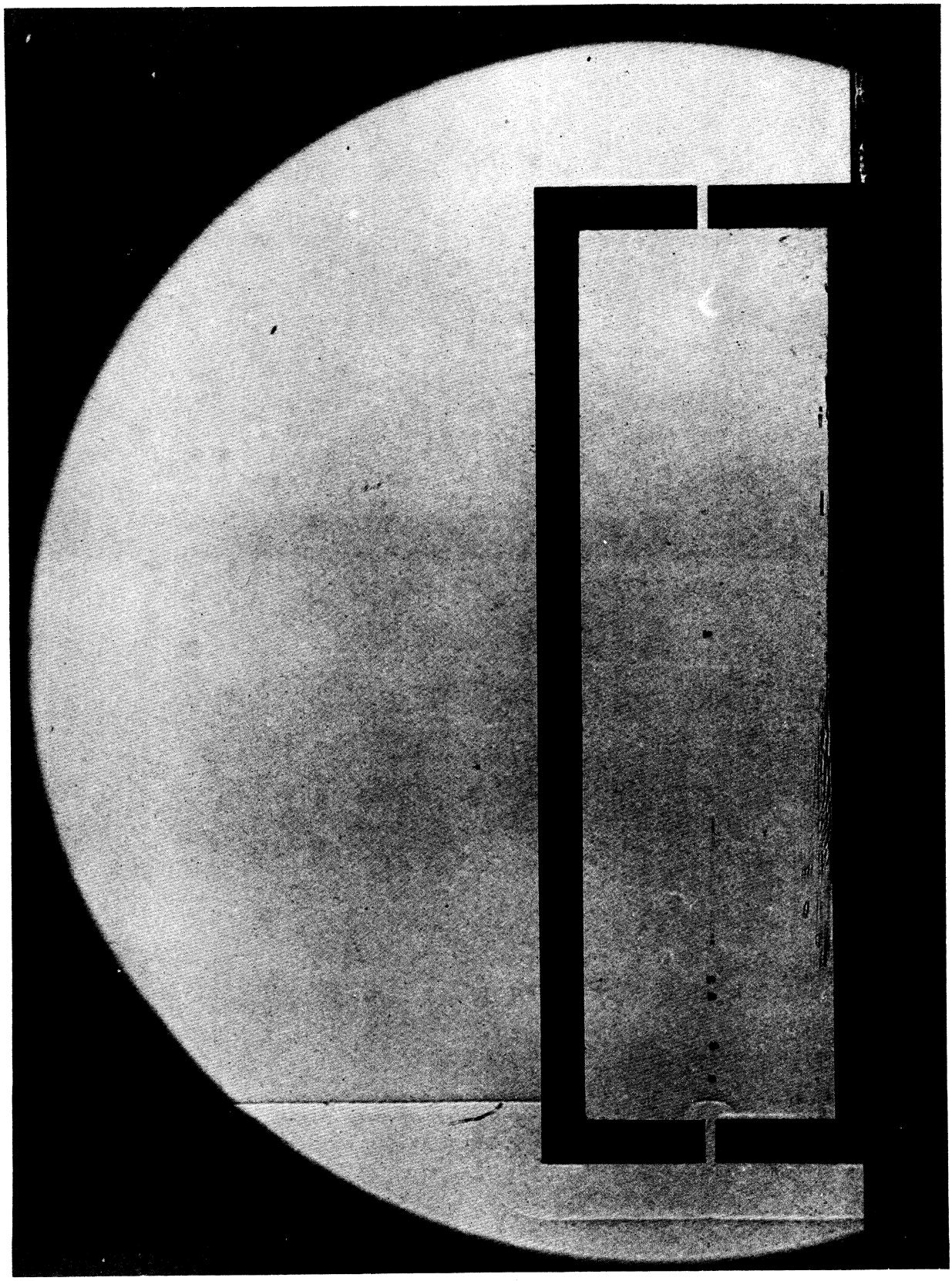

t = 20

Figure 31

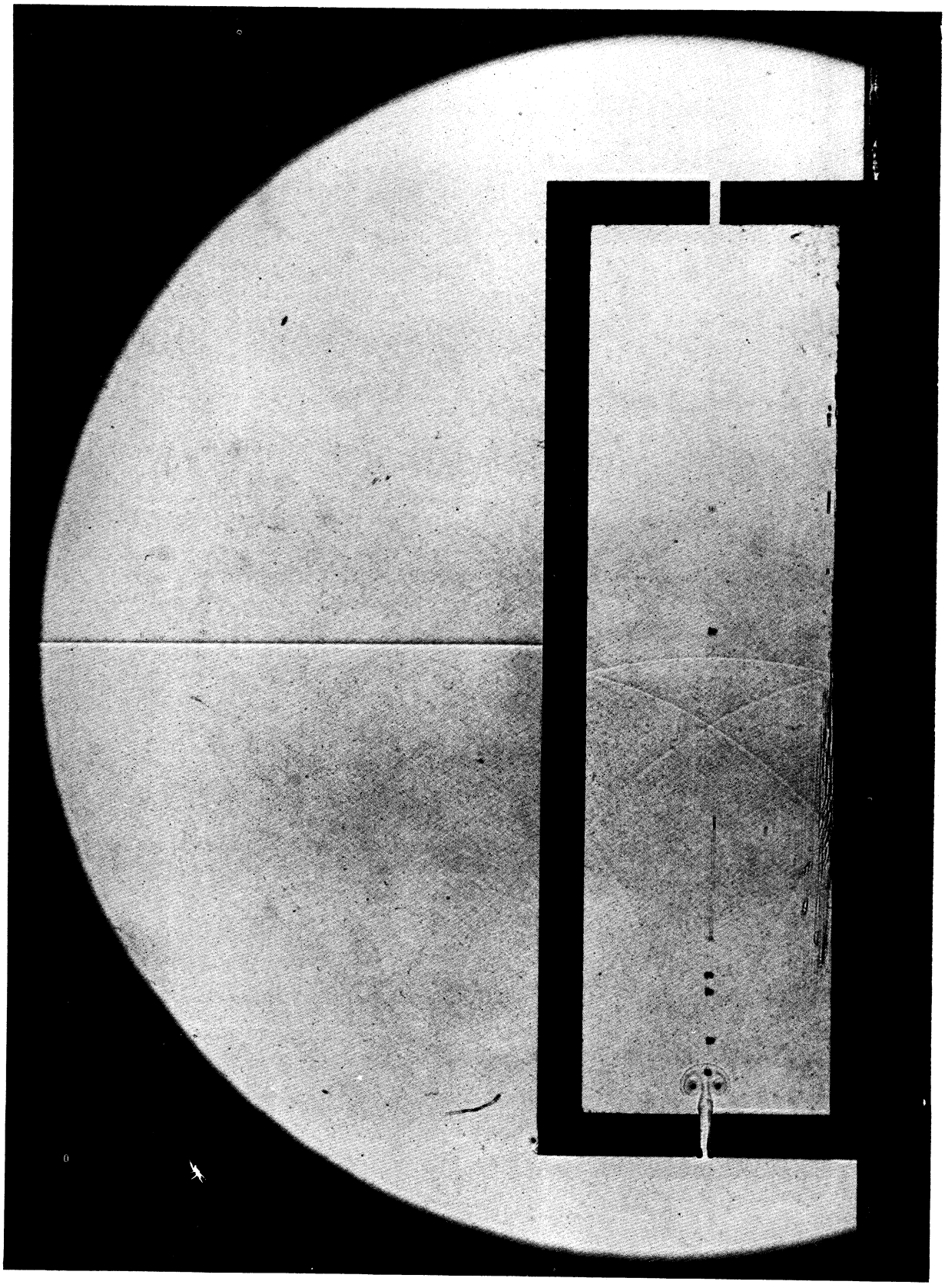

t = 168

Figure 32

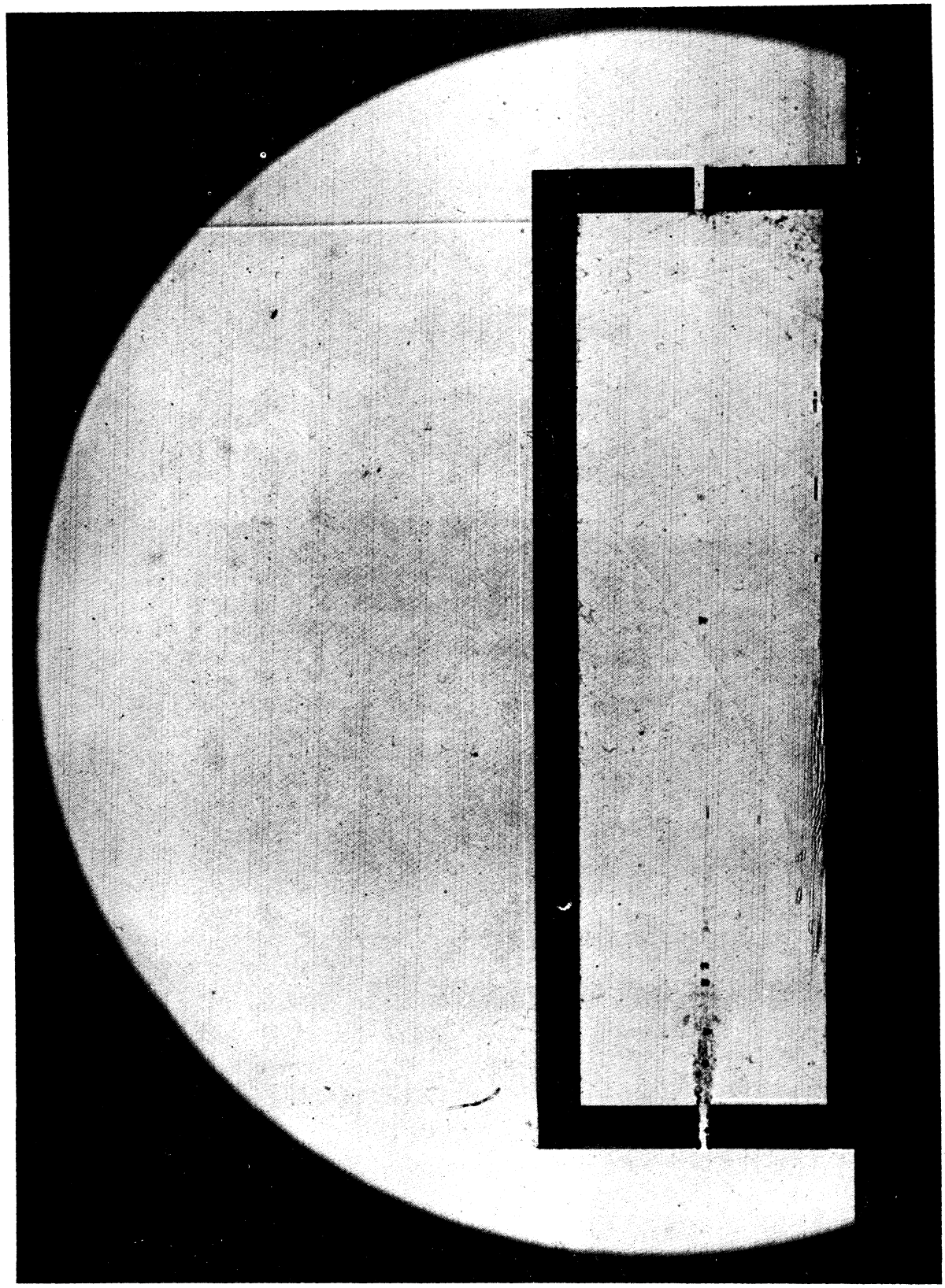

t = 305

Figure 33

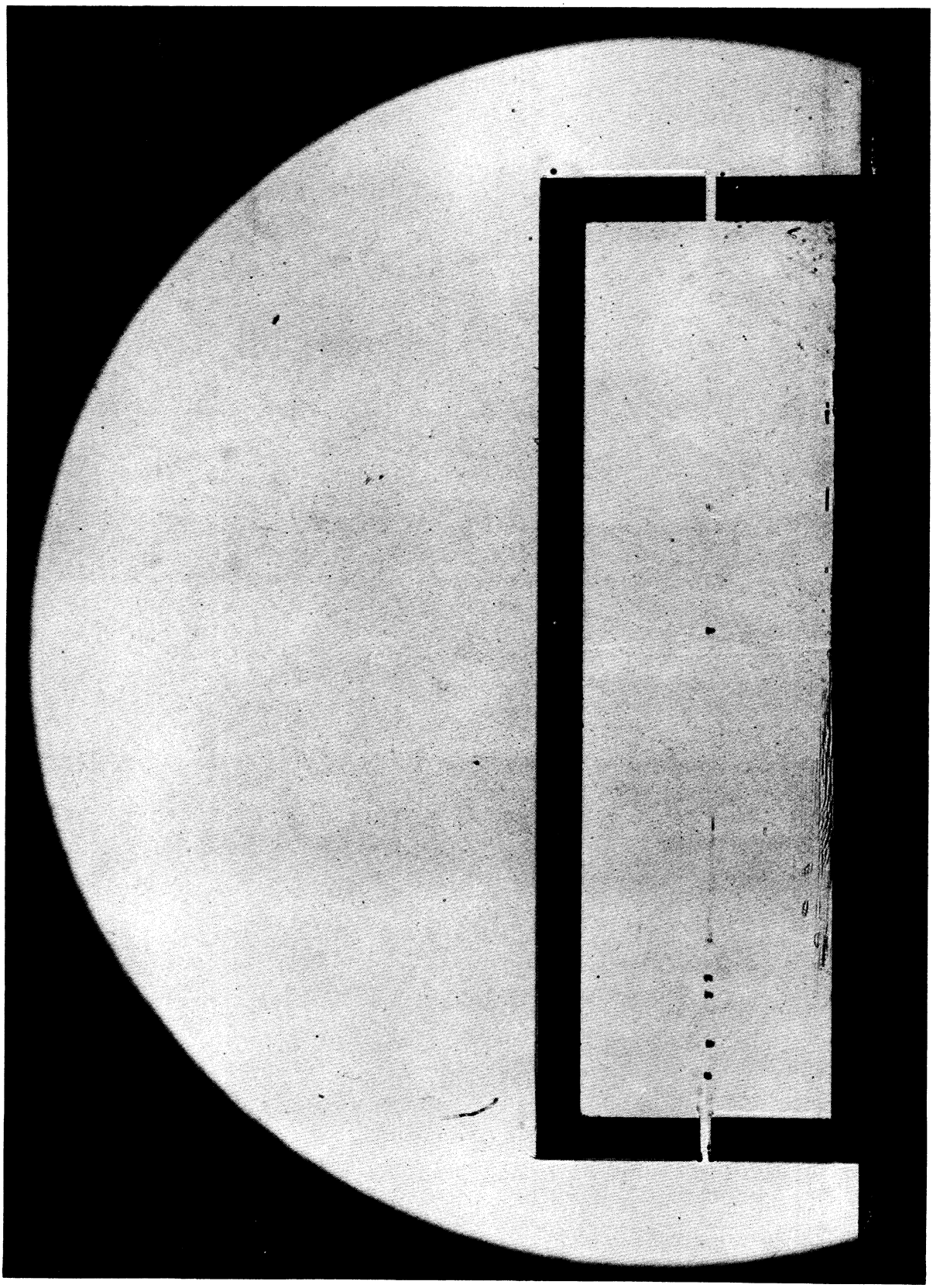

t = 460

Figure 34

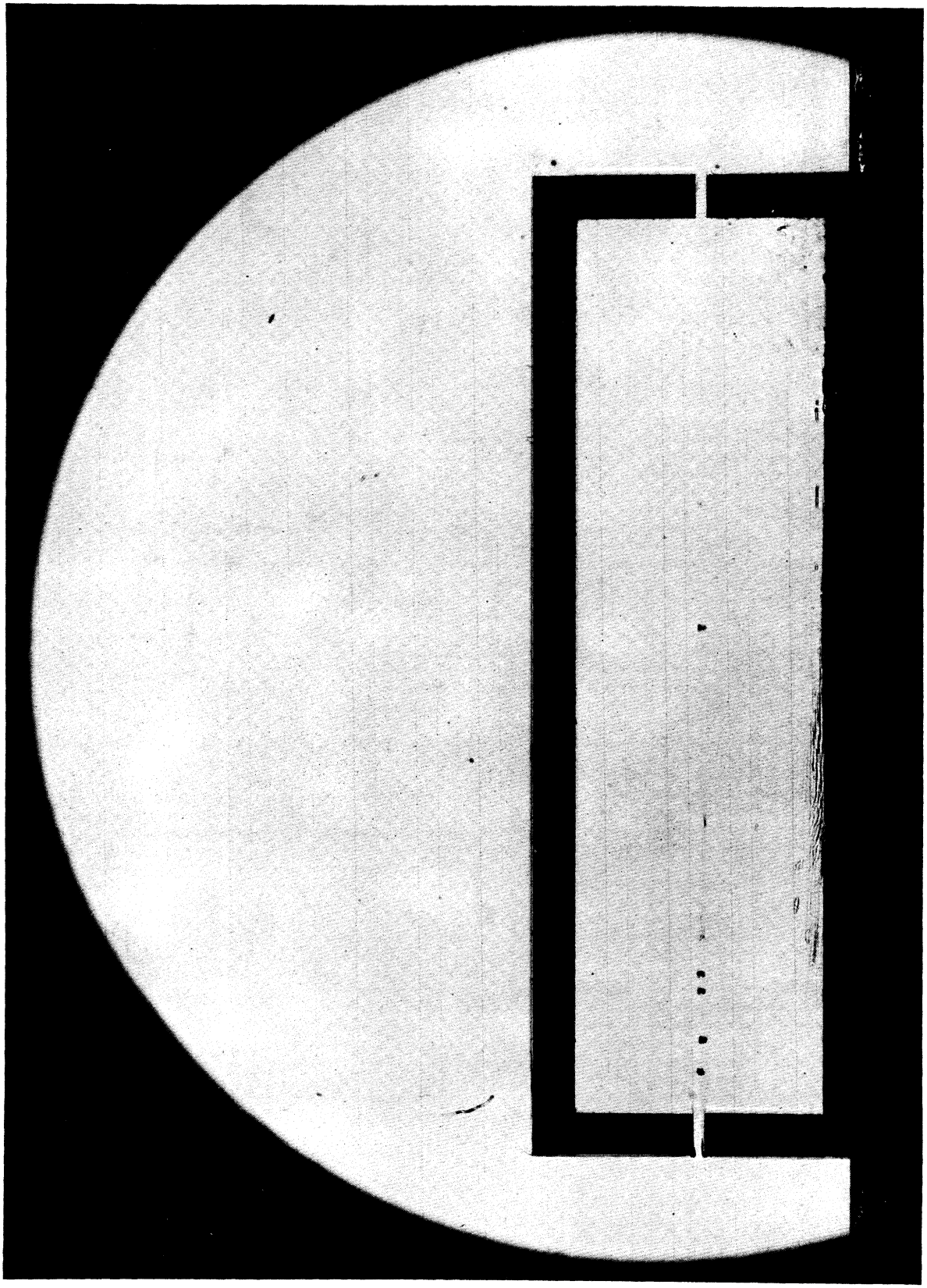

t = 574

Figure 35

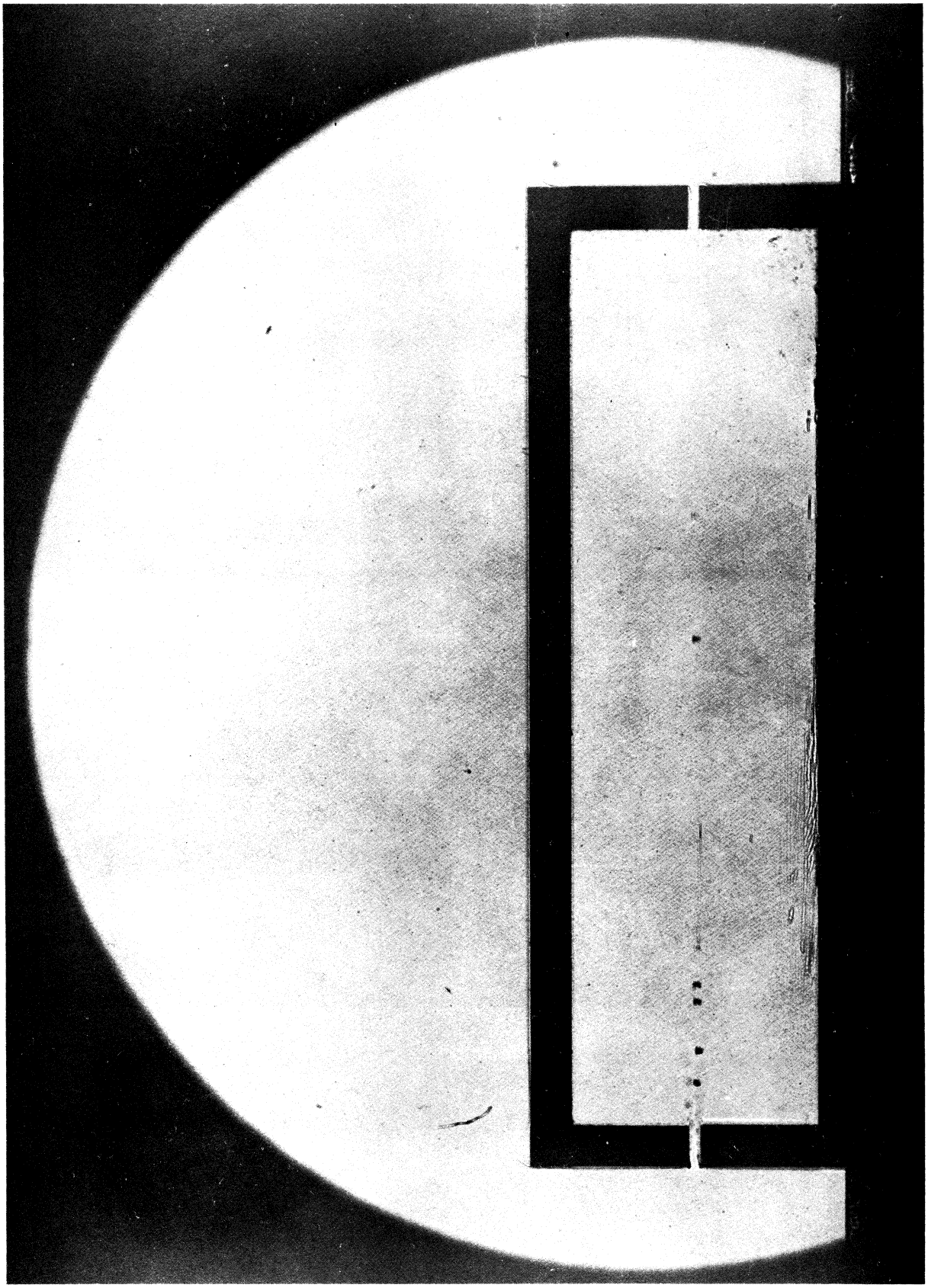

t = 709

Figure 36

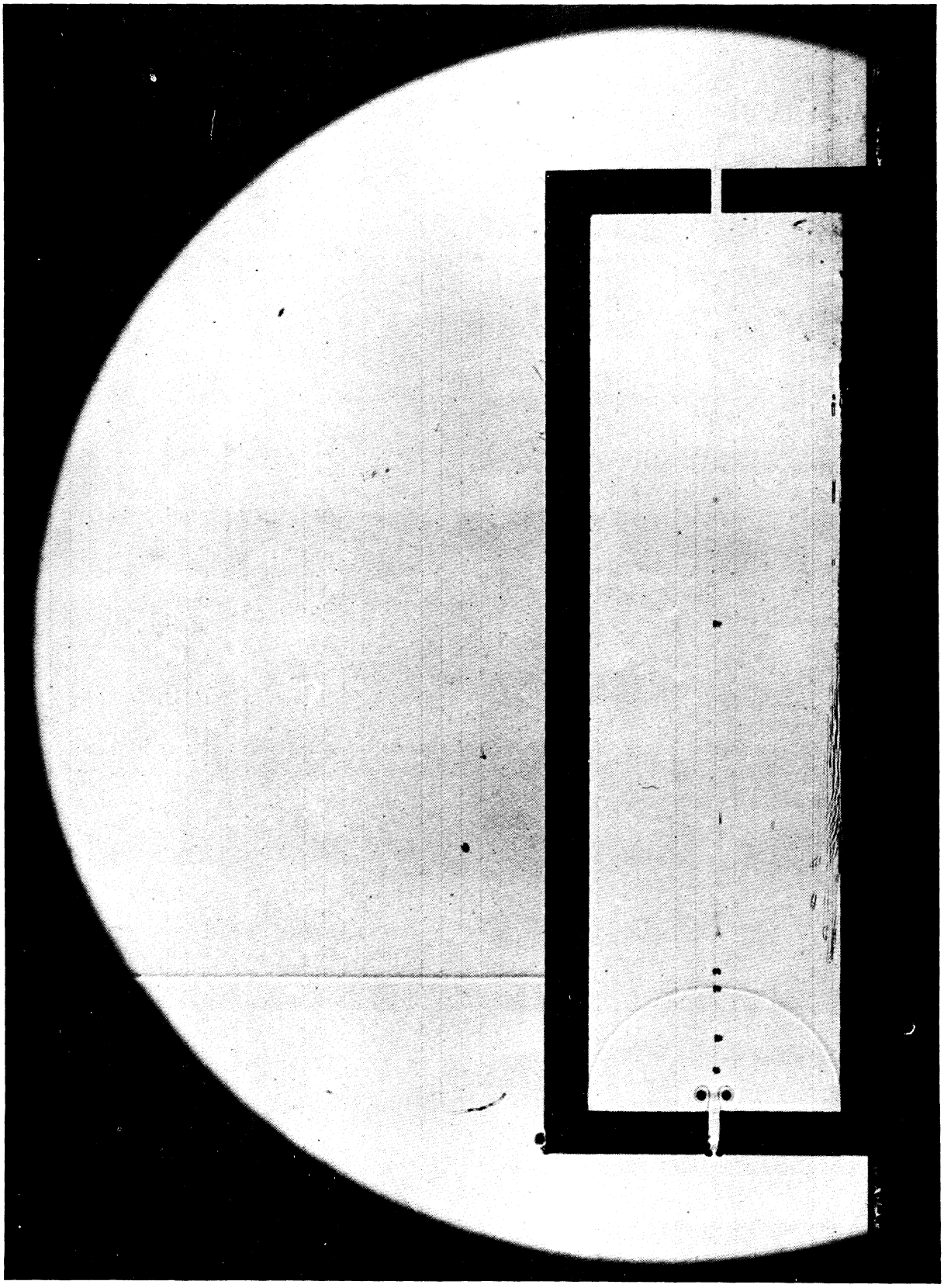

t = 52

Figure 37

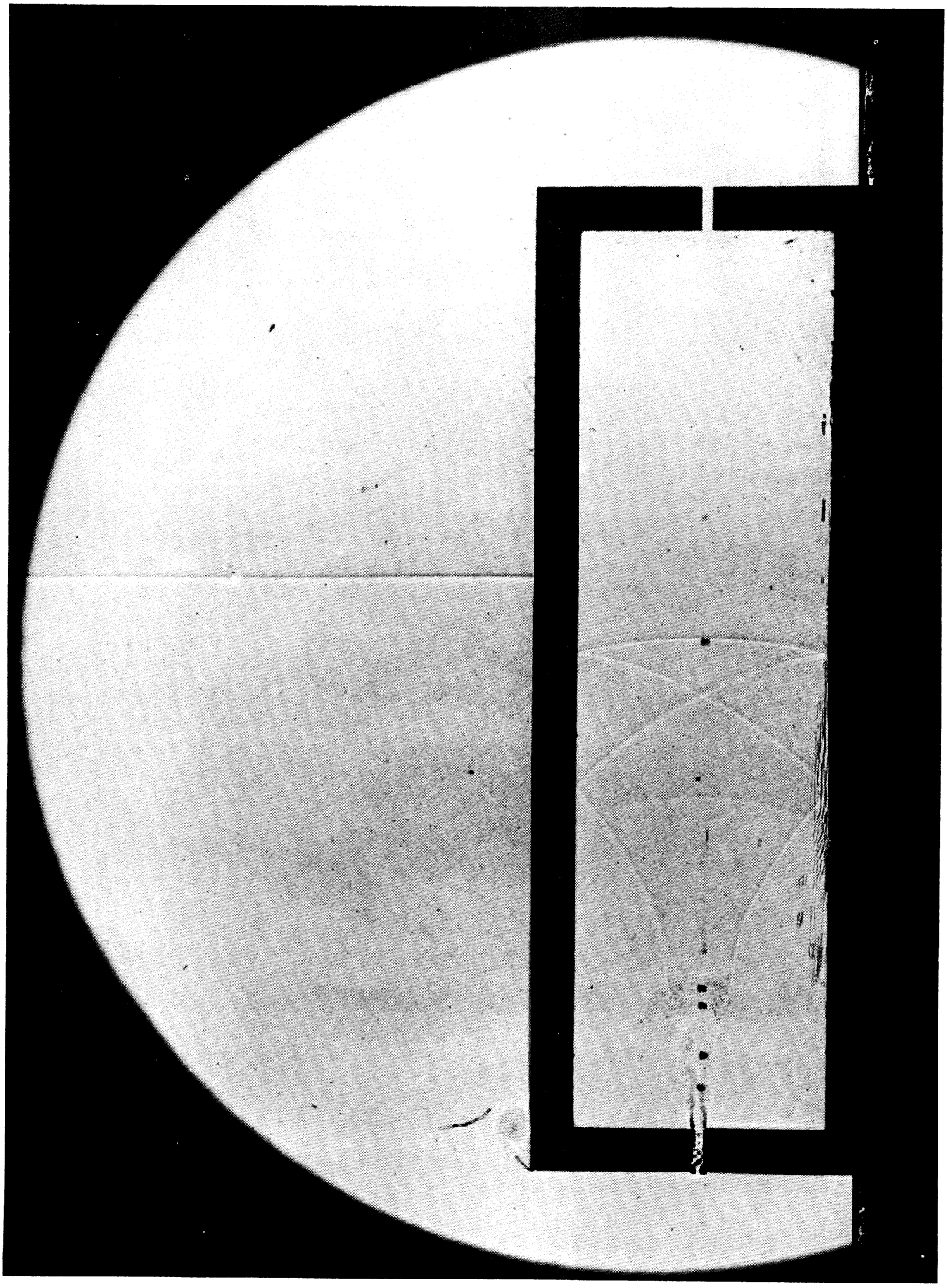

t = 171

Figure 38

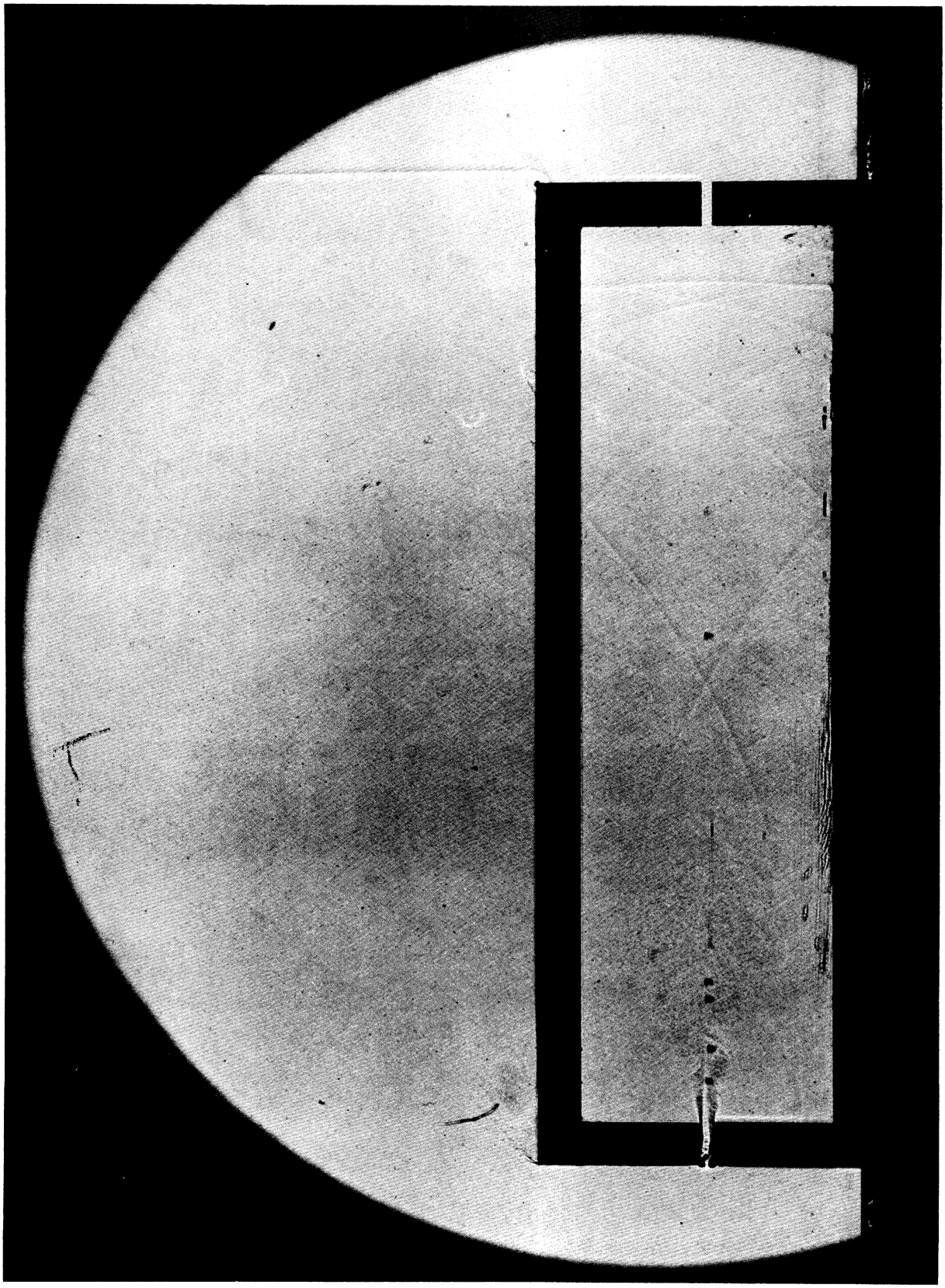

t = 292

Figure 39

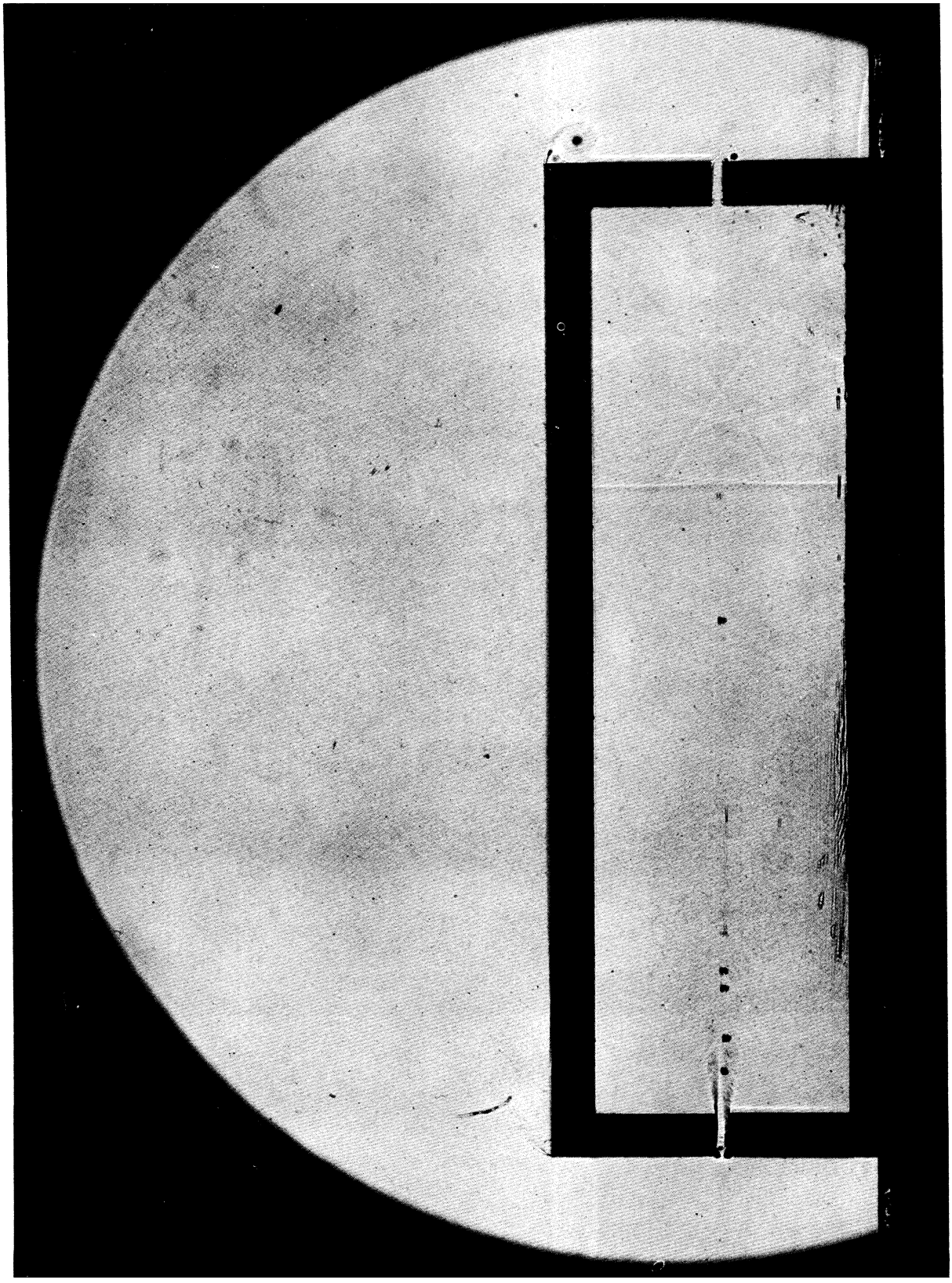

t = 402

Figure 40

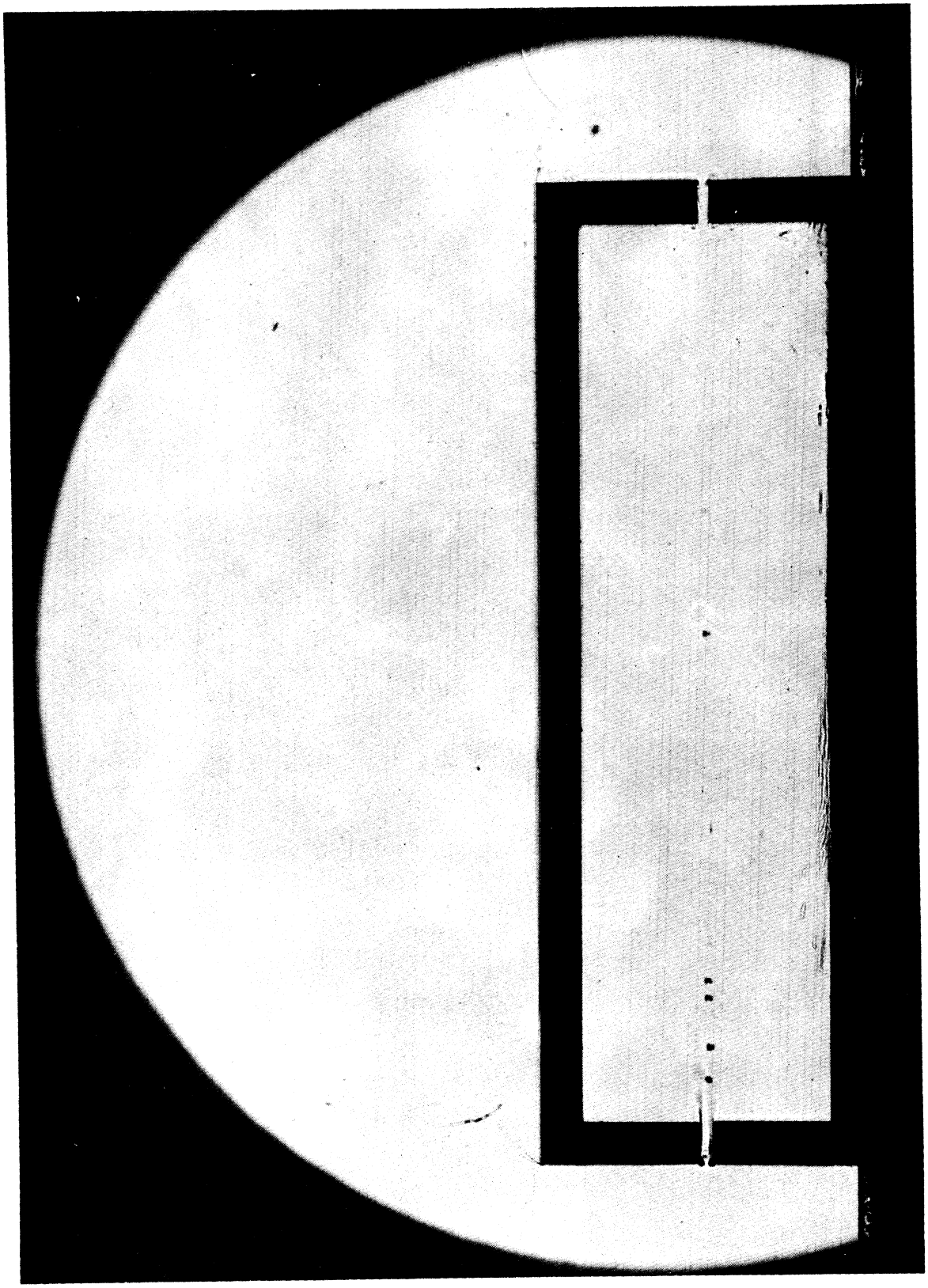

t = 537

Figure 41

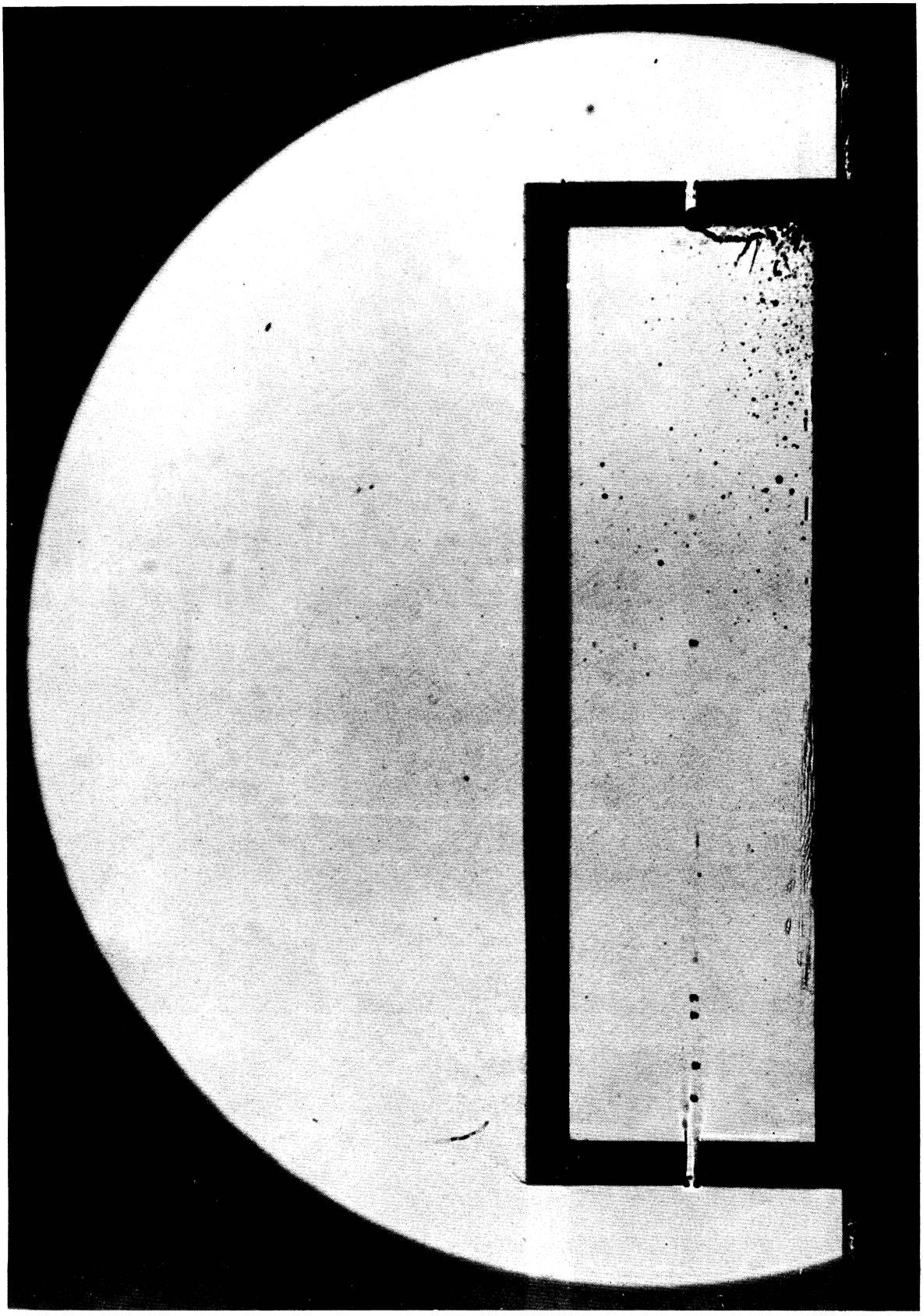

t = 610

Figure 42

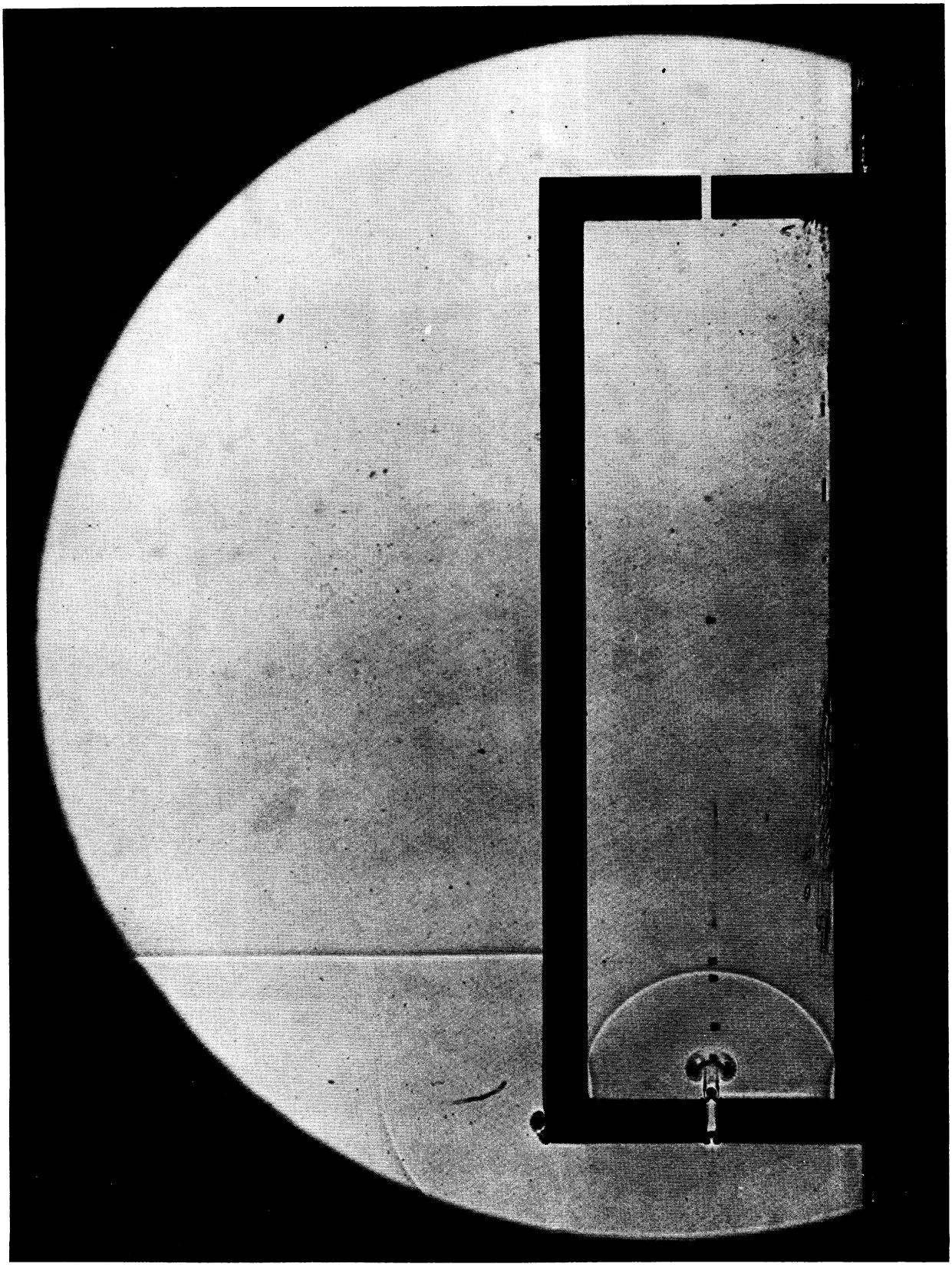

t = 49

Figure 43

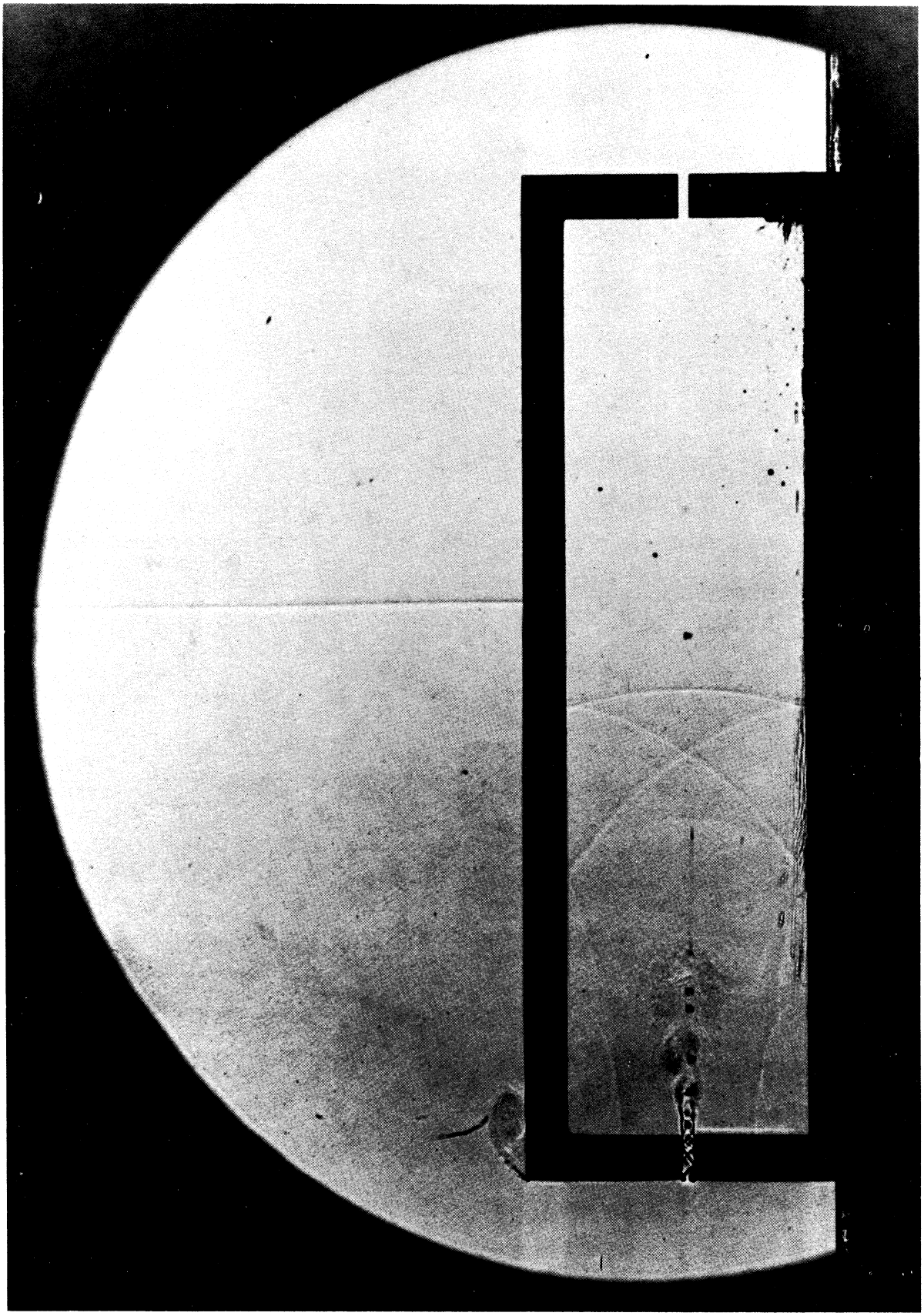

t = 145

Figure 44

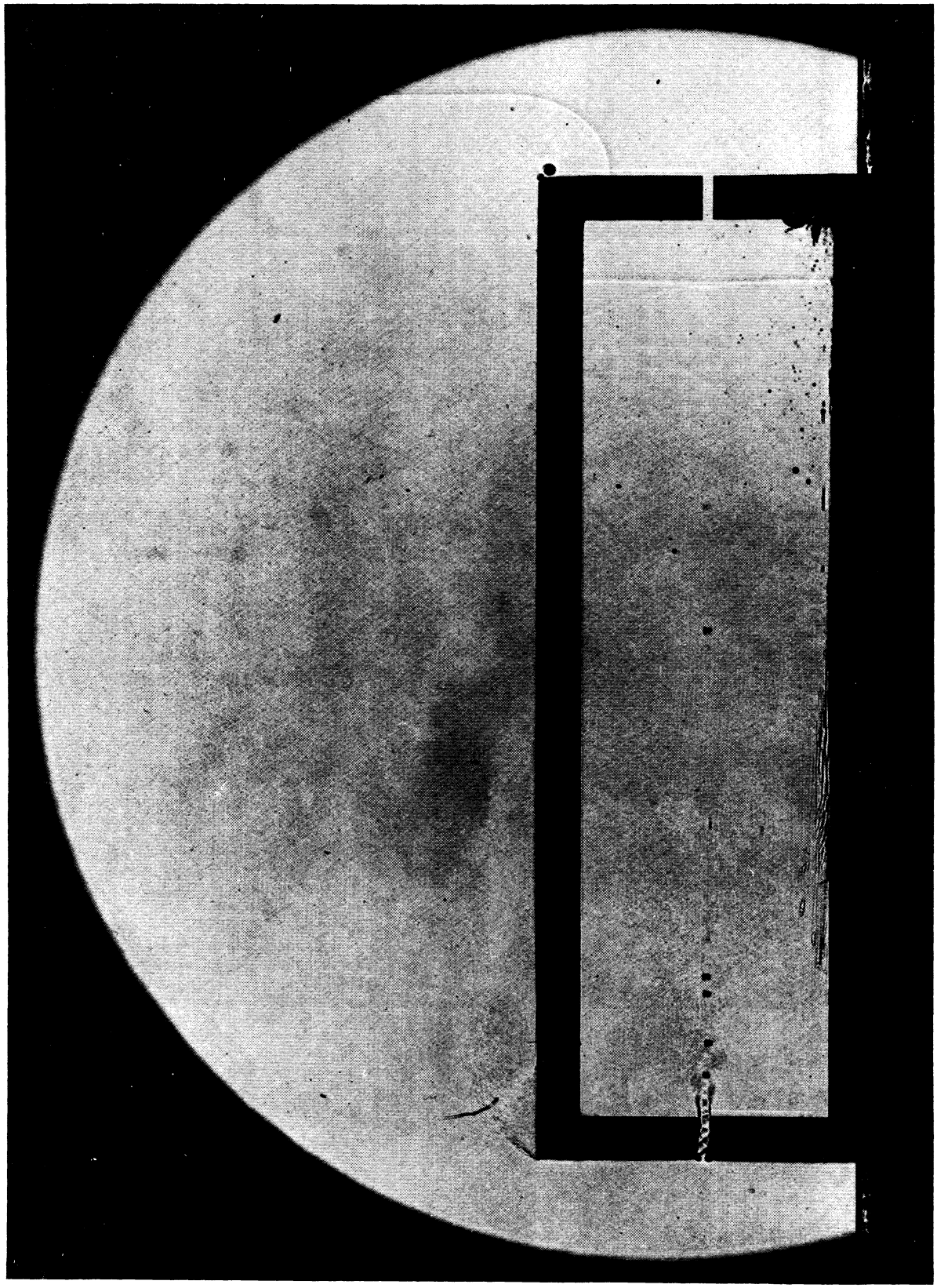

t = 276

Figure 45

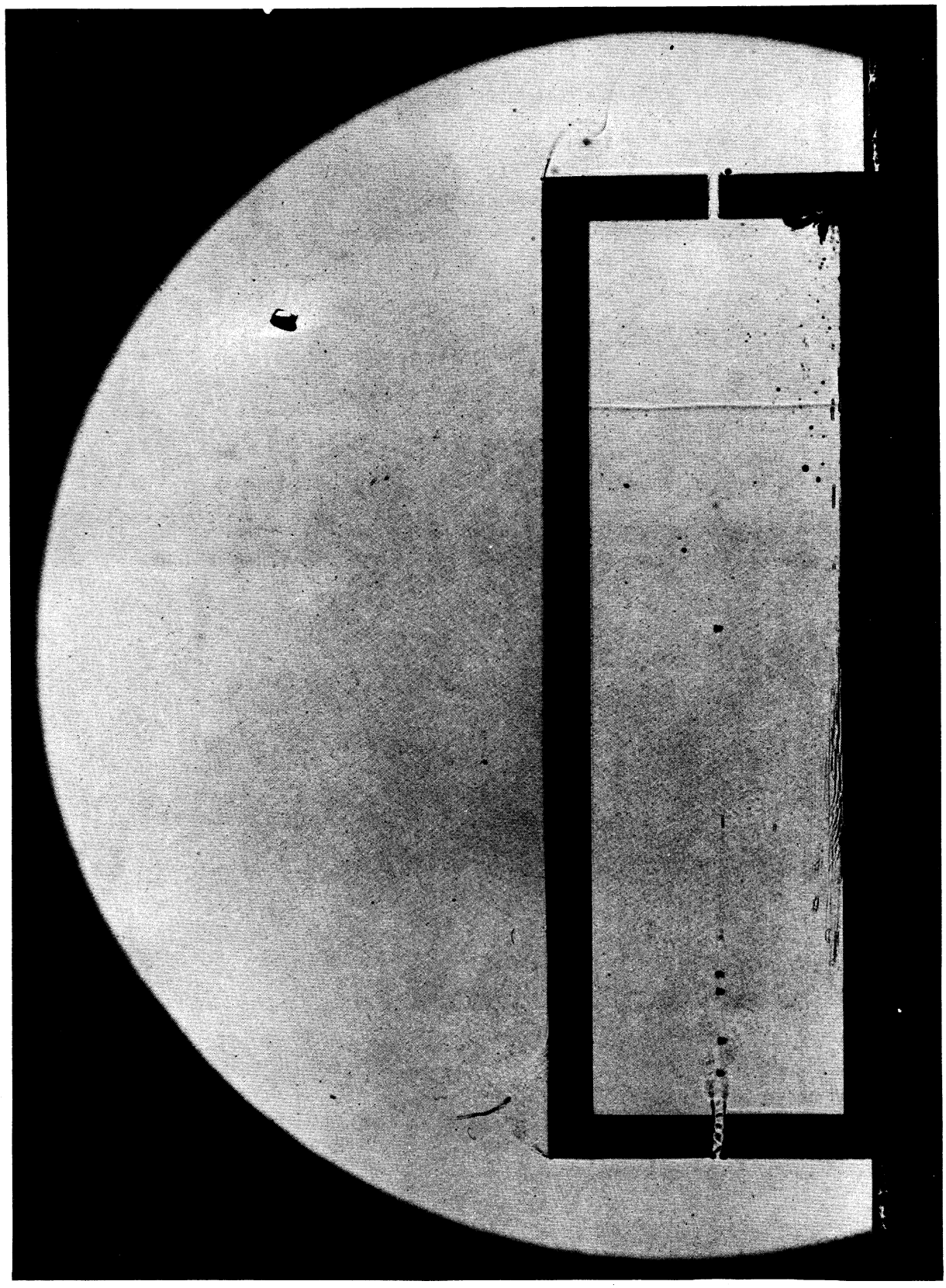

t = 356

Figure 46

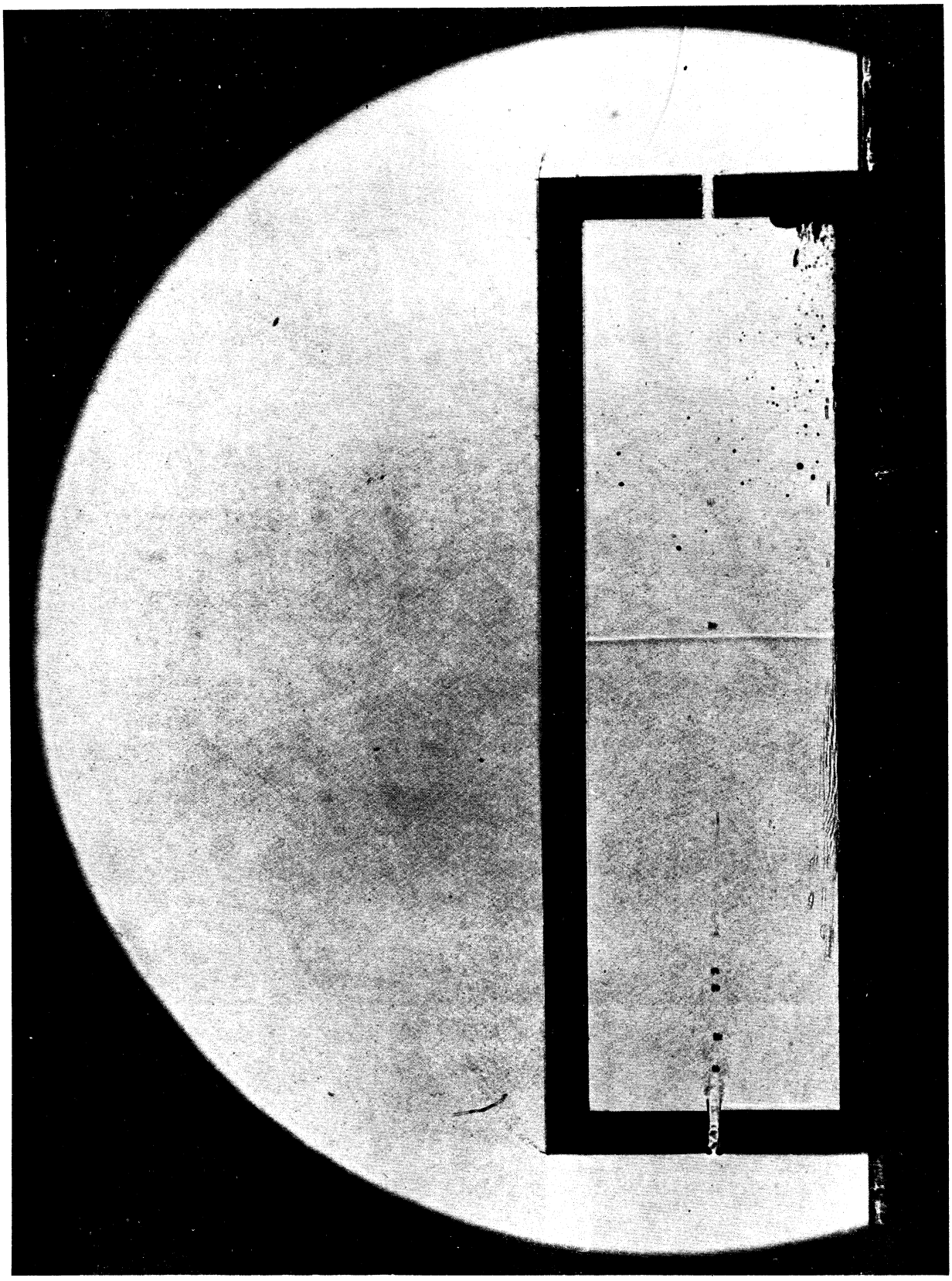

t = 439

Figure 47

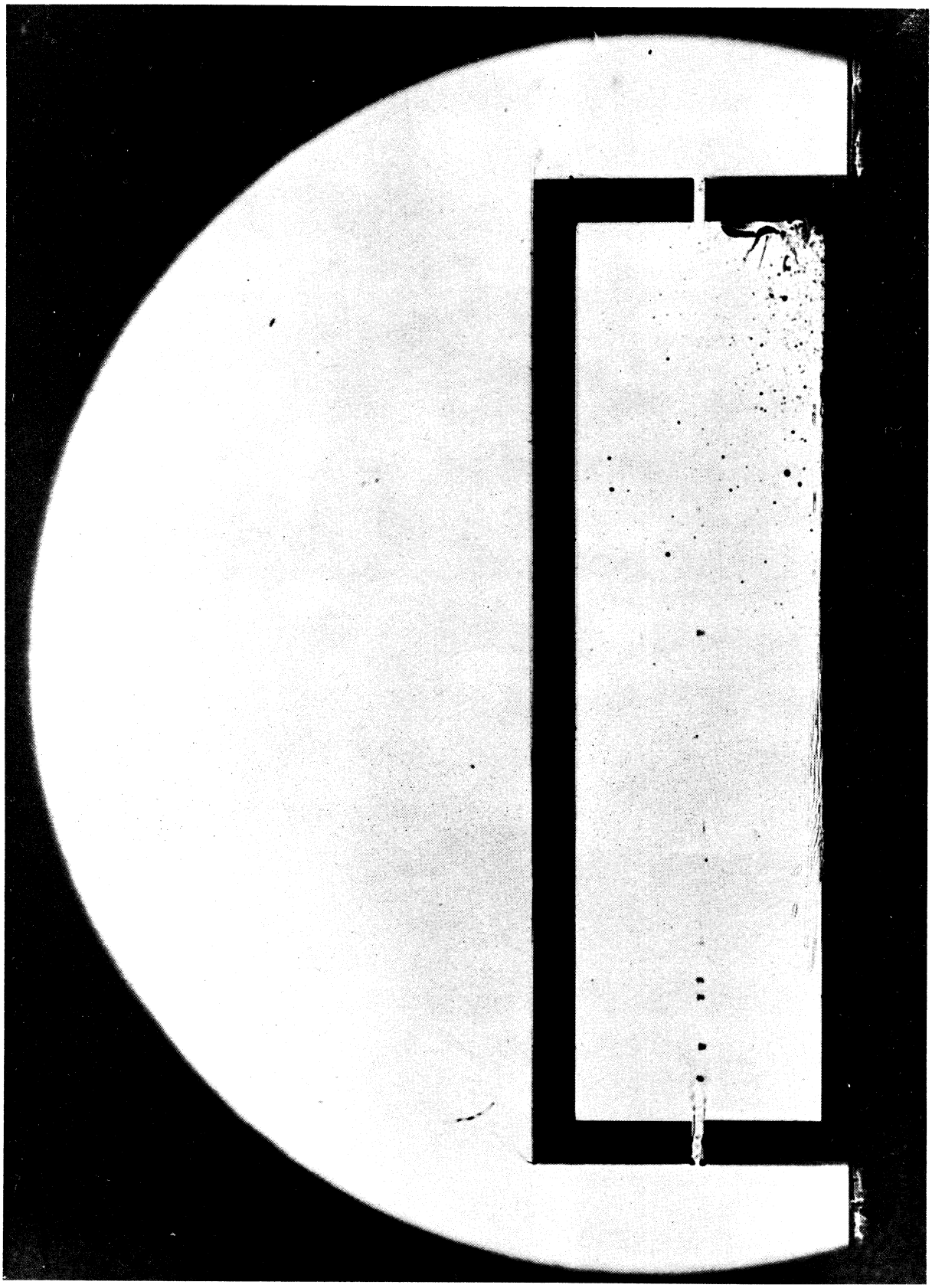

t = 514

Figure 48